

Summer 2019

ENHANCING THE EFFICIENCY OF ELECTROKINETIC REMEDIATION THROUGH THE USE OF COMPLEXING AGENTS

Timothy Driscoll

Follow this and additional works at: https://digitalcommons.mtech.edu/grad_rsch

 Part of the [Civil and Environmental Engineering Commons](#)

ENHANCING THE EFFICIENCY OF ELECTROKINETIC REMEDIATION
THROUGH THE USE OF COMPLEXING AGENTS

by
Timothy Driscoll

A thesis submitted in partial fulfillment of the
requirements for the degree of

Masters of Science:
Environmental Engineering

Montana Tech

June 2019



Abstract

Electrokinetic remediation was assessed as a viable remediation technology for heavy metal contamination modeled after contamination present in Butte, MT caused by over a century of hard rock mining. The remediation technology was assessed at a laboratory scale using copper sulfate (CuSO_4) as a model compound of mine tailing contamination, and an artificial soil to control for variables outside the scope of work. This thesis designed a laboratory scale experiment that produced consistent results and could be easily repeated. The system design also included a method for managing the waste material produced during experiments. Following the experimental design, this thesis evaluated the effect of several complexing agents on the transport rates of copper ions (Cu^{2+}) in an electrokinetic system. Chloride (Cl^-), bromide (Br^-), ammonia (NH_3), and ethylenediaminetetraacetic acid (EDTA) were used to complex copper ions, originally hydrated with water molecules. A total of 17 experiments were conducted during this thesis. Transport rates were calculated using real-time direct current measurements and inductively coupled plasma (ICP) analysis data. Previous studies suggested that the transport of the complexed ions was directly proportional to their complex radii. However, in this thesis, the size to transport rate relationship was not observed, and depletion/enrichment rates varied within experiments. Depletion and enrichment were defined as the percent change of copper mass in the electrode compartment from initial to final conditions. The largest enrichment rates were observed in the CuSO_4 experiments at 0.082 mg s^{-1} while the largest depletion rates were observed in the EDTA experiments at 0.093 mg s^{-1} . Changes in pH caused by the electrolysis of the electrodes is a likely underlying factor behind the mixed results, as these pH changes play a large role in altering the solubility of the metals in solution.

Keywords: electrokinetic remediation, complexing agents, heavy metal remediation, mine impacted soil, ion transport.

Dedication

I would like to dedicate this these to my wife Miki Anderson, and my parents Larry and Maureen Driscoll. Their kindness, patience, love and support are what has kept me motivated throughout this project and allowed me to reach the point that I am at today.
Thank you.

Acknowledgements

I would like to thank Xufei Yang for all the help he gave me during this thesis. Xufei created the program that allowed me to collect real time current readings during the experiments and designed a way to run two reactors at a time. Thank you to my committee members for their input, patience, and expertise. I would also like to thank Jackie Hedval for all the amazing help with CAD design. I would like to thank MT Tech and Water and Environmental Technologies for everything that I have learned over the last three years of education and working, as well as thank them for their continued patience with what has been a busy and hectic schedule. Finally, I would like to thank Jeanne Larson for all of her support from day one and all the hard work she puts into the Environmental Engineering Department.

Table of Contents

ABSTRACT	II
DEDICATION	III
ACKNOWLEDGEMENTS	IV
LIST OF TABLES.....	VII
LIST OF FIGURES.....	VIII
LIST OF EQUATIONS	X
1. INTRODUCTION	1
1.1. <i>Heavy Metal Contamination in Butte, MT</i>	1
1.2. <i>Electrokinetic Remediation</i>	4
1.3. <i>Thesis Goals and Objectives</i>	16
2. METHODS AND MATERIALS	18
2.1. <i>Experimental Design</i>	18
2.1.1. Reactor Design.....	18
2.1.2. Experimental sand medium.....	21
2.1.3. Reactor Loading.....	22
2.1.4. Solution Preparation.....	23
2.1.5. Reactor experiments	24
2.1.6. Decontamination.....	26
2.1.7. Waste Management	27
2.2. <i>Experimental Data and Analysis</i>	28
2.2.1. In-situ current monitoring.....	28
2.2.2. Reactor sampling.....	30
2.2.3. Data Analysis	31
3. RESULTS.....	33

3.1.	<i>Experimental Results</i>	33
3.2.	<i>Data Analysis Results</i>	42
3.2.1.	Current Measurements	43
3.2.2.	Electrode Compartment Depletion	46
3.2.3.	Electrode Compartment Enrichment	48
3.2.4.	Observed Copper Transportation Rates	50
4.	DISCUSSION.....	58
4.1.	<i>Discussion on Experimental Design</i>	58
4.2.	<i>The Effect of Complexing Agents on Transport Rates</i>	59
4.3.	<i>Recommendations</i>	64
4.4.	<i>Future Work</i>	65
4.5.	<i>Conclusion</i>	66
5.	APPENDIX A	1
6.	REFERENCES CITED.....	1

List of Tables

Table I. Total Copper Concentration ICP Results.38

Table II. Apparent rate constants used to calculate Enrichment and Depletion.49

List of Figures

Figure 1. Illustration of an Idealized Electrokinetic System.....	7
Figure 2. Copper Hexaaqua Complex.....	14
Figure 3. Copper Complexes used for EK Experiments.....	15
Figure 4. EK Reactor Blueprint.	19
Figure 5. Permeable Barriers used to Separate Electrode Compartments from Soil.	20
Figure 6. Laboratory Experiment Setup and Reactors.....	26
Figure 7. Wire Diagram of EK experiments.	29
Figure 8. Cathode Mass Change during 48 hour experiments.....	34
Figure 9. Anode Mass Change during 48 hour experiments.	35
Figure 10. Photo of electrodes following Baseline Experiments.....	36
Figure 11. Copper Plating on Positive EDTA Electrode after polishing.....	37
Figure 12. Electrode compartment percent enrichment.	40
Figure 13. Electrode Compartment percent depletion.	40
Figure 14. Copper Mass in the Electrode Chambers and soil column.....	42
Figure 15. Copper Hexahydrate Current Readings.....	44
Figure 16. Copper-EDTA Current Readings.	44
Figure 17. Copper-HCl Current Readings.	45
Figure 18. Copper-HBr Current Readings.....	45
Figure 19. Copper-NH ₃ Current Readings.....	46
Figure 20. Modeled Depletion for each Complex Type.	47
Figure 21. Modeled Enrichment for each Complex Type.	48

Figure 22. Baseline Concentration Changes.....	51
Figure 23. EDTA Complexed Copper Concentrations Changes.....	52
Figure 24. HCl Complexed Copper Concentrations Changes.....	53
Figure 25. HBr Complexed Copper Concentrations Changes.....	54
Figure 26. NH ₃ Complexed Copper Concentrations Changes.....	55
Figure 27. Anode Compartment Mass Change (mg s ⁻¹).....	56
Figure 28. Cathode Compartment Mass Change (mg s ⁻¹).....	56
Figure 29. Right- NH ₃ Reactor Precipitation. Left- HBr Reactor Precipitation.....	61
Figure 30. Pourbaix Diagram of the Speciation of Copper Ions.....	63

List of Equations

Equation 1 Current in Electrolytic Solution.....	11
Equation 2 Anodic Oxygen Evolution.....	12
Equation 3 Cathodic Hydrogen Evolution.....	12
Equation 4 Copper EDTA Complex.....	24
Equation 5 Copper Bromide Complex.....	24
Equation 6 Copper Chloride Complex.....	24
Equation 7 Copper Ammonia Complex.....	24
Equation 8 Ohms Law.....	29
Equation 9 Electrode Compartment Concentration.....	31
Equation 10 Concentration Change.....	31
Equation 11 Mass change per second.....	32
Equation 12 Percent Change.....	39

1. Introduction

This section provides a brief background on the heavy metal contamination present in Butte, MT. An understanding of the contamination present in the shallow aquifer in Butte, MT is key to appreciating the thesis goal behind this work, regarding the importance of electrokinetic remediation. Following the history of heavy metal contamination in Butte, this section will give a literature review of electrokinetic remediation technology at its current state.

1.1. Heavy Metal Contamination in Butte, MT

Butte, MT is located in Southwest Montana, west of the Continental Divide. Butte sits on top of a granitic pluton intrusion of Cretaceous Butte Quartz Monzonite that is rich in hydrothermally precipitated sulfite copper minerals, as well as smaller concentrations of silver and gold minerals. Weathered granite and alluvial deposits from nearby mountains form most of the surface lithology and the upper shallow aquifer. Since being originally settled in the mid-1800s, mining has occurred in Butte, at small or large scales for the better part of the past 150 years. During the early 1900s, copper extraction in Butte grew to a tremendous scale in order to meet the copper demand of an increasingly industrializing nation. The grand scale of mining has had significant impacts on the local environment and water quality. Originally, mining was done underground, where miners would follow ore deposits, and haul ore to the surface where it would be later smelted and concentrated. Underneath the surface of Butte is an estimated 16,000 km of mine shafts, reaching to depths of 1.6 km and covering an area of 20 km². During the mid-1900s underground mining was transitioned into open pit mining, and the formation of the

Berkeley Pit began. An estimated 700 million tons of rock were removed from 1953 to 1983, when the open pit operations ended.¹

Mining activity has produced a number of environmental issues in Butte. Numerous dewatering pumps were used to lower the groundwater table and allow miners access to the deep ore deposits. This also formed a cone of depression, or sink, in the aquifer, creating a groundwater divide around the mine working. Similar to a water shed divide, groundwater on either side of the divide would flow into, or away from the cone of depression. Following the mining closure in 1983, the dewatering pumps were powered down. With the pumps shut off, the groundwater level began to return to its initial level, filling in the cone of depression, and flooding the existing mine working in the process.² Acid mine drainage was created when the groundwater reacted with the sulfite minerals in the oxygen enriched environment of the mine tunnels, and previously dewatered subsurface. As the groundwater level continued to rise, the acid rock drainage flooded the existing mine tunnels and began to pool in the Berkeley Pit. The water level of the Berkeley Pit continues to rise today and has presented a number of challenges to the ground water quality in Butte, MT.³ A leading concern regarding the Berkeley Pit is in keeping the water level below what is referred to as the critical level. The critical level is the ground water elevation at which the Pit is no longer a sink for contaminated groundwater in the area. When the water table is above this level, the groundwater divide no longer exists and the

¹ Christopher H Gammons, John J. Metesh, and Terence E. Duaiame, *An overview of the mining history and geology of Butte, Montana* (Mine Water and the Environment, 2006), 72,

² Andy Davis, and Ashenberg Daniel, *The aqueous geochemistry of the Berkeley Pit, Butte, Montana, USA* (Applied Geochemistry, 1989), 23-36.

³ Christopher H Gammons, and James P. Madison, *Contaminated alluvial ground water in the butte summit valley* (Mine Water and the Environment, 2006), 126.

acidic groundwater in the surrounding area, which is highly contaminated with heavy metals, will flow outward and into Silver-Bow Creek, a headwater of the Clark Fork River. Water treatment plants have been constructed to treat the water in the acid lake and maintain the water level below the critical level.

Butte faces another, less visible, source of heavy metal contamination resulting from over a century of mining operations. During the underground mining of early 1900s, ore was brought to the surface, where it was crushed, smelted, and concentrated before being shipped offsite by railcar. This was a very energy intensive process and resulted in a great deal of waste rock, or mine tailings. In Butte, many of the smelters were located along Silver-Bow Creek, a small creek that flows through the community. These smelters disposed of the mine tailings by using the flow of the creek to carry away some of the finer material, and by impounding the larger waste rock along the stream beds.⁴ This practice was done at a time where little to no environmental regulations existed and not only was the waste rock impounded along the streamside, but mine waste was often used as a fill material for construction projects in the community. This resulted in a widespread, poorly documented heavy metal contamination throughout uptown Butte. These mine tailings pose a large risk to the environmental and human health of the community because they are pervasive and close to the surface. As a result, runoff from precipitation events conveys large loads of dissolved heavy metals into Silver-Bow Creek.⁵ Unlike the underground contamination resulting from the flooded mine shafts, the mine tailings at Butte's surface are hydrologically connected to the surface water of Butte. As left untreated, the heavy metals in the

⁴ Christopher H Gammons, and James P. Madison, *Contaminated alluvial ground*, 126-129.

⁵ Christopher H Gammons, Christopher L. Shope, and Terence E. Duaine, *A 24-h Investigation of the Hydrogeochemistry of Baseflow and Stormwater in an Urban Area Impacted by Mining: Butte, Montana*. (Hydrological Processes: An International Journal, 2005), 2740.

mine tailings mobilize into Silver-Bow Creek. Some remediation efforts are already underway at the time of writing this thesis. The tailings impoundments from the historic Parrot Smelter, located along present-day Civic Center Road, are currently being remediated by excavation. The project involves using X-ray fluorescence to screen the clean subsurface from the mine tailings. The tailings are then trucked offsite to a leach pad near the Berkeley Pit, where they are hydrologically isolated because of the groundwater divide. The Parrot Tailings are of such a massive scale that an ex-situ remediation technique such as excavation is the only practical solution. However, there are many areas in Butte that are equally contaminated, but at a smaller scale, and are not suited for excavation. There are areas of uptown Butte where tailings overlain with existing buildings and infrastructure would make ex-situ remediation difficult. The goal of this thesis is to explore the viability of using electrokinetic remediation for in-situ remediation of heavy metal contamination present in the shallow aquifer under Butte, Montana.

1.2. Electrokinetic Remediation

Heavy metal contaminated soils are a pressing issue for many communities around the world. Since 1980, and the enactment of the Comprehensive Environmental Response, Compensation, and Liability Act (CERCLA), over 1000 locations in the United States have been listed on the National Priority List (NPL), i.e., granted as Superfund sites. Many of them were identified for heavy metal contamination.⁶ Various technologies exist today for the removal of heavy metals in subsurface soils. The main type of remediation is *ex-situ* remediation. These remediation projects involve excavating and removing the contamination from the subsurface

⁶ Superfund: National priorities list (NPL). in United States Government [database online]. 2017 [cited 01/10 2018]. Available from <https://www.epa.gov/superfund/superfund-national-priorities-list-npl>.

and transporting it offsite to treatment facilities. This type of remediation is effective in that it allows projects to directly access the contamination and remove it in large volumes. While simple in concept, logistical issues regarding heavy machinery, community relations, and safety issues need to be addressed during these types of work. In addition, excavation can be difficult if the contamination is overlain with existing infrastructure. Conversely, heavy metal contamination can be treated using *in-situ* remediation techniques. *In-situ* remediation involving heavy metals primarily consists of pumping the contaminated groundwater out of the subsurface, and treating it using pH adjustments to cause the metals to drop out of solution. This type of remediation is carried out by treating the contamination in place, without the need for excavation.^{7,8} Improving the efficiency of contaminant removal is crucial to making *in-situ* remediation a more viable cleanup strategy.

Electrokinetic (EK) remediation is a relatively new technology that has the potential to enhance the removal of heavy metals from contaminated soil and groundwater. EK remediation relies on transportation of ionic species under an electric energy gradient, created by applying a voltage across the contaminated subsurface using electrodes submerged in the aquifer. The energy gradient causes species in the water to migrate towards either the anode or cathode in one of three ways: electro-osmosis, electromigration, or electrophoresis. Electro-osmosis is the bulk movement of water along an electric gradient, electromigration is the movement of ions along an electric gradient, and electrophoresis is the movement of charged particles along an electric

⁷ Zhiting Yao, Jinhui Li, Henghua Xie, and Conghai Yu, *Review on remediation technologies of soil contaminated by heavy metals*. (Procedia Environmental Sciences, 2012), 722-729.

⁸ CN Mulligan, RN Yong, and BF Gibbs *Remediation technologies for metal-contaminated soils and groundwater: An evaluation*, (Engineering Geology, 2001), 200.

gradient.⁹ Figure 1, below is an illustration of a typical full scale EK system. The top of this illustration shows electrodes housed in well casing, submerged in a contaminated aquifer. The wells are energized by a power source, depicted as battery. The bottom of the illustration depicts how mass is transported in an EK system, either by electrophoresis, electroosmotic flow, or electromigration. For heavy metal soil remediation, the dominant mechanism is electromigration.¹⁰

⁹ Jurate Virkutyte, Mika Sillanpää, and Petri Latostenmaa *Electrokinetic soil remediation—critical overview* (Science of the Total Environment, 2002) 98-101.

¹⁰ Akram Alshwabkeh, and Yalcin B. Acar, *Electrokinetic remediation. II: Theoretical model* (Journal of Geotechnical Engineering, 1996), 187.

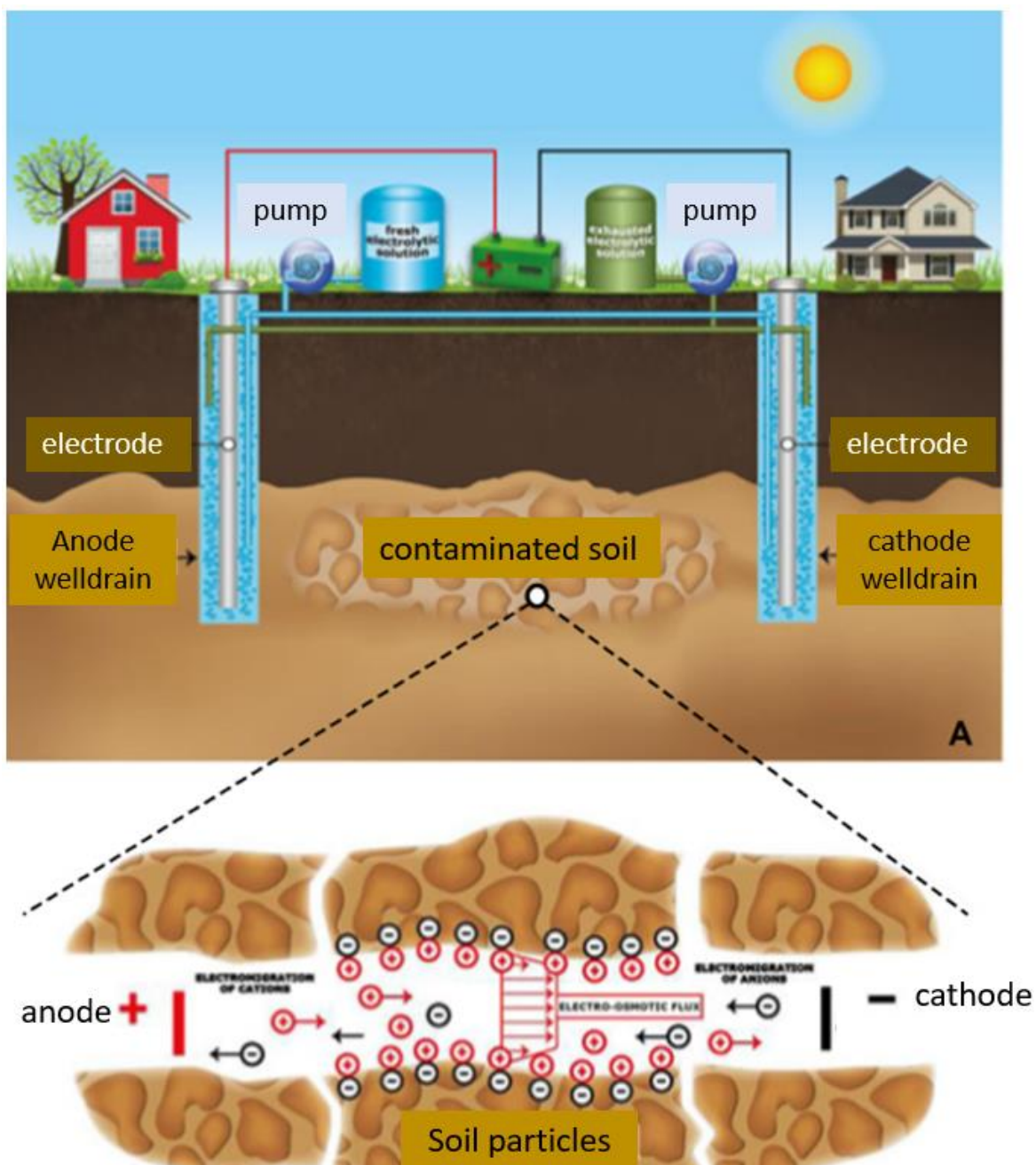


Figure 1. Illustration of an Idealized Electrokinetic System.

¹¹ Courtesy of David Rosetolato et al. 2015.

¹¹ Davide Rosetolato, Roberto Bagatin, and Sergio Ferro, *Electrokinetic remediation of soils polluted by heavy metals (mercury in particular)*, (Chemical Engineering Journal 264 (2015)), 17.

In a full-scale system, the electrodes would be inside of a well casing screened inside of the contamination. As the EK proceeds, the ionic species are concentrated in the volume of water near the electrodes of opposite charge. Since the water immediately surrounding the well/electrode arrangement contains a high concentration of heavy metals, it can then be pumped out for further disposal. The enrichment of heavy metal ions results in a greater contaminant removal per unit of pumped groundwater; and the pumped flowrate is closely related to the operating cost of a remediation project. Other removal mechanisms of heavy metals include electroplating onto the electrode, if reductive conditions and ionic species allow, and precipitation in the form of metal hydroxides. Both electroplating and precipitation depend on the redox potential of the species, and the pH of the solution surrounding the electrode. Precipitation is often viewed as an undesirable process during EK remediation. Although it removes metals from a groundwater solution, precipitation immobilizes the contamination in the system and makes further removal difficult.¹²

Soils contaminated with organic pollutants can also be remediated by EK. In projects targeting organic contaminants, the electric current breaks down organic compounds as well as concentrates them in the well casing, to a lesser degree because organic compounds are mostly nonpolar, and therefore less susceptible to electromigration.^{13,14}

¹² Albert T. Yeung, *Milestone developments, myths, and future directions of electrokinetic remediation* (Separation and Purification Technology, 2011), 124.

¹³ AB Ribeiro, JM Rodriguez-Maroto, EP Mateus, and H. Gomes, *Removal of organic contaminants from soils by an electrokinetic process: The case of atrazine.: Experimental and modeling.* (Chemosphere, 2005), 1230.

¹⁴ Gordon Yang, and Yu-Wen Long, *Removal and degradation of phenol in a saturated flow by in-situ electrokinetic remediation and fenton-like process.* (1999), 260.

As aforementioned, the electrodes in an EK system are typically housed in a well casing, where the groundwater solution is either directly accessible to the electrode through a screened well casing. In some cases, the electrode is separated by an intermediate material between the electrode and the groundwater that acts as a filter. Some of these filters are salt bridges that function as pH controls by limiting or neutralizing the spread of H^+ or OH^- ions. Other types of filters are comprised of reactive materials, such as Zero-Valent Iron, react with the metal ions as they travel toward the electrodes, causing metal hydroxide precipitation to occur inside the filter that can then be removed and replaced.¹⁵

EK systems can not only serve as a standalone remediation solution but also augment other remediation techniques, such as *in-situ* chemical and biochemical oxidation.¹⁶ The electric potential gradients caused by EK, specifically electromigration and electrophoresis, allow better accessibility to contamination locked in the pore spaces of soil particles with low permeability, such as clays. Without an electric gradient, a solution will travel along the path of least resistance, and only enters porous media of low permeability through molecular diffusion, which can be very slow. Traditionally, these soil particles lock away pollutants, and are responsible for a long-term, constant release of compounds that can make it difficult and costly to achieve cleanup goals. With the addition of an electrical gradient, the rate of transport in or out of these low permeable zones is increased. Under an electric potential, compounds can be leached out of low permeability particles to react with remediation reagents, likewise the reagents can be

¹⁵ Shuning Zhao, Li Fan, Mingyuan Zhou, Xuefeng Zhu, and Xiuli Li, *Remediation of copper contaminated kaolin by electrokinetics coupled with permeable reactive barrier*, (Procedia Environmental Sciences, 2016), 274-279.

¹⁶ Xuhui Mao, James Wang, Ali Ciblak, Evan E. Cox, Charlotte Riis, Mads Terkelsen, David B. Gent, and Akram N. Alshwabkeh, *Electrokinetic-enhanced bioaugmentation for remediation of chlorinated solvents contaminated clay*, (Journal of Hazardous Materials, 2012), 311-313.

delivered into the low permeable particles. EK systems have also been hybridized with biological remediation systems with some success. A biological remediation system relies on bacteria to degrade pollutants. EK has been shown to increase the metabolic rates of bacteria in breaking down organic contaminants.^{17,18}

For a standard EK system to be successful, a site needs to meet certain criteria. The contaminant transport rates induced by electroosmosis, electromigration, and electrophoresis are relatively small. For these to have any effect on the groundwater solutions, the groundwater velocity needs to be slow, otherwise, the groundwater bulk flow (caused by a gravitational gradient) outweighs the EK-induced contaminant transport. When the groundwater velocity is high, EK can be used as an *ex-situ* remediation technique, where soils are excavated and EK is carried out in a holding tank where system functions can be easily controlled.¹⁹ Similarly, molecular diffusion needs to be low for electromigration to be significant. Transport caused by diffusion is always in the direction of high concentration to low concentration. Electromigration transport is in the opposite direction, in that it concentrates ions near the poles. Diffusion rates are typically orders of magnitude lower than electromigration rates, and diffusion can be neglected. However, in highly porous systems, such as a low clay content, sandy subsurface, the effect of diffusion may be more prominent.²⁰

¹⁷ Ahmed Chowdhury, IA, Jason I. Gerhard, David Reynolds, Brent E. Sleep, and Denis M. O'Carroll, *Electrokinetic-enhanced permanganate delivery and remediation of contaminated low permeability porous media* (Water Research, 2017), 215-218.

¹⁸ Xuhui Mao, James Wang, Ali Ciblak, Evan E. Cox, Charlotte Riis, Mads Terkelsen, David B. Gent, and Akram N. Alshawabkeh, *Electrokinetic-enhanced bioaugmentation*, (2012), 313.

¹⁹ MT Ammami, Florence Portet-Koltalo, Ahmed Benamar, C. Duclairoir-Poc, H. Wang, and F. Le Derf *Application of biosurfactants and periodic voltage gradient for enhanced electrokinetic remediation of metals and PAHs in dredged marine sediments* (Chemosphere, 2015), 2.

²⁰ Akram Alshawabkeh, and Yalcin B. Acar, *Electrokinetic remediation. II* (1996), 189.

EK systems require that the targeted subsurface soil have high electrical conductivity. This can be an obstacle if the target contaminant is above the water table, or is an organic pollutant, but this difficulty does not typically arise in metal polluted groundwater remediation projects. Metal contamination is often a result from industrial or mining activity and is often accompanied by low pH conditions. Acidic groundwater solutions typically result in highly mobile metal species with high electrical conductivity.²¹

Changes in electrical properties can be used to monitor the performance of the system. As an EK system evolves, metal ions migrate towards the electrodes and the ion concentration in the bulk groundwater (in the spacing between electrodes) becomes depleted. Current in an electrolytic solution is defined as the motion of charged particles by the equation:

$$i = F \sum_i z_i N_i \quad \text{Equation 1 Current in Electrolytic Solution.}$$

where i is the current density ($A\ cm^{-2}$), F is Faraday's Constant ($A\ mol^{-1}$), z_i is the number of proton charges carried by an ion, and N_i is the flux density of ion i ($mol\ cm^{-2}$).²² From this principle, it can be seen that the current decreases proportionally with decreases in the flux of ions traveling across the reactor. Current is easy to measure in an EK system and is often monitored during studies as a real-time indication of performance.²³ In full scale remediation systems, a current drop is often used as an indication to pump out the concentrates from well casing, as ions are at their highest concentration. Full scale systems are de-energized at this point

²¹ Jurate Virkutyte, Mika Sillanpää, and Petri Latostenmaa *Electrokinetic soil remediation* (2002) 101-102.

²² John Newman, and Karen E. Thomas-Alyea, *Electrochemical systems* (John Wiley & Sons, 2012), 272.

²³ Davide Rosestolato, Roberto Bagatin, and Sergio Ferro *Electrokinetic remediation of soils polluted by heavy metals (mercury in particular)* (Chemical Engineering Journal, 2015) 19-21.

to allow the groundwater solution to re-equilibrate. Often, the polarity of the electrodes will be reversed on the next system turn-on. This helps the system re-equilibrate, as well as helps to neutralize the pH fronts produced from the previous run.²⁴

A primary site condition that can affect EK removal rates is pH. Applying an electric current across water produces water electrolysis at the anode and cathode, as follows:



Water electrolysis creates what are referred to as acidic and basic fronts, which migrate away from the anode and cathode respectively. These fronts are particularly significant in groundwater solutions with low buffering capacity. A basic front can greatly degrade removal efficiency. As positively charged ionic species migrate to the cathode they encounter increasingly basic conditions and can precipitate out of solution as metal hydroxides or oxides.²⁵ Not only does this result in less contaminant reaching the well casing, but it also reduces the electric conductivity of the soil.²⁶ The pH fronts are sometimes addressed²⁶ by using ion membranes that block the flow of OH⁻ ions outside of the well. As shown in Figure 1, some systems have addressed the pH

²⁴ Sandu, Ciprian, Marius Popescu, Emilio Rosales, Marta Pazos, Gabriel Lazar, and M. Ángeles Sanromán. "Electrokinetic oxidant soil flushing: a solution for in situ remediation of hydrocarbons polluted soils." *Journal of Electroanalytical Chemistry* 799 (2017): 1-8.

²⁵ Ramasubramania Iyer, *Electrokinetic remediation*, (Particulate science and technology 19, no. 3, 2001), 223.

²⁶ Sandu, Ciprian, Marius Popescu, Emilio Rosales, Marta Pazos, Gabriel Lazar, and M. Ángeles Sanromán. "Electrokinetic oxidant soil flushing: a solution for in situ remediation of hydrocarbons polluted soils." *Journal of Electroanalytical Chemistry* 799 (2017): 1-8.

problem by continually mixing the electrode fluid between the cathode and anode chambers, which helps to neutralize the pH conditions.²⁷

Electrokinetic remediation systems are typically energized using a constant voltage gradient of 1 V/cm, in other words, a system with an electrode spacing of 1 meter would be run with a voltage drop of 100 V across the electrodes.²⁸ Less traditional systems maintain a constant current between the electrodes, altering the voltage as the system evolves. EK systems have been operated by solar, wind or other passive energy generating devices, although these systems have not been fully researched at a pilot scale study. These systems have been successfully operated under much lower voltage gradients and could be used in areas where electricity is not readily available or is cost-prohibitive.²⁹

EK remediation has a wide range of applications and there are many areas of research that have not yet been explored. EK remediation technology has existed for decades but until several drawbacks are addressed, it will not have practical uses in real-world cleanup projects. A voltage gradient of 1 volt per cm electrode spacing is the typical energy gradient. This makes it difficult to use EK remediation on large area projects. Also, as with other *in-situ* remediation technologies, removal rates are so much slower compared to the more intrusive method of excavation.³⁰

²⁷ Yalcin B. Acar, Robert J. Gale, Akram N. Alshawabkeh, Robert E. Marks, Susheel Puppala, Mark Bricka, and Randy Parker. *Electrokinetic remediation: basics and technology status* (Journal of hazardous materials 40, no. 2 ,1995) 119.

²⁸ Yalcin B. Acar, Robert J. Gale, Akram N. Alshawabkeh, Robert E. Marks, Susheel Puppala, Mark Bricka, and Randy Parker. *Electrokinetic remediation* (1995) 127.

²⁹ F.L. Souza, C. Saéz, J. Llanos, M. R. V. Lanza, P. Cañizares, and M. A. Rodrigo. *Solar-powered electrokinetic remediation for the treatment of soil polluted with the herbicide 2, 4-D* (Electrochimica Acta 190 2016), 371-377.

³⁰ CN Mulligan, RN Yong, and BF Gibbs *Remediation technologies* (2001), 200.

As previously stated, the driving transport mechanism for heavy metals in an EK system is electromigration. Electromigration is the movement of the ions inside the solution, rather than the movement of the solution itself. This transport mechanism is a function of the charge on the ion, the tortuosity of the flow path created by the porous media, and the size of the ion. A key factor to improving the efficiency, and therefore the applicability, of electrokinetic remediation is improving the rate of ion transport. Properties such as the porosity, conductivity, and tortuosity of the subsurface are intrinsic to the subsurface, are site specific, and cannot be easily altered. However, the charge and size of the target ion can be altered with the use of complexing agents.

The size of a metal ion in an aqueous solution is determined by what is called the hydrated radius, or the radius of the ion and the molecules, typically water, that are weakly bonded to it in solution through electrostatic forces. The size of the hydrated radius is proportional to the density of charge of the ion itself. In other words, a small ion will have a larger hydrated radius than a larger ion with the same charge because the dense charge of the smaller ion is able to attract more water molecules. For example, the inner radius of a copper ion hydrated with water molecules will consist of one copper ion (Cu^{2+}) hydrated with six water molecules (H_2O), oriented so that the negative pole of the water molecule, the oxygen, is nearest the copper ion. Figure 2 below is an illustration of this molecule.

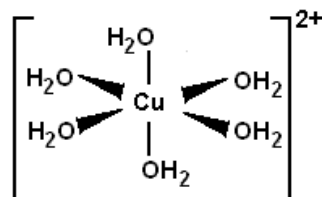


Figure 2. Copper Hexaqua Complex.

The six water molecules form monodentate ligand bonds with the copper ion. This molecule, known as a copper hexaqua complex has an octahedron geometry with an extension

along the Z-axis due to Jahn Teller Elongation. The diameter of this ion along the long axis of this complex is 4.72 angstroms.

By visualizing the ion and its hydration shell as a rigid unit, Stokes Law would imply that when the ion moves within a solution, this shell creates a drag force in the direction opposite of movement. While the size of the hydraulic radius and the ionic mobility are not monotonically proportional, generally speaking, the smaller the hydrated radii, the smaller the drag force, and therefore the larger the ionic mobility within a solution.³¹ This thesis sets out to determine if copper ions with smaller complex radii display faster and therefore more efficient transport rates in an electrokinetic reactor. Copper ions were originally hydrated with water molecules, which were subsequently replaced with Cl^- , Br^- , NH_3 , and ethylenediaminetetraacetic acid (EDTA), illustrated below in Figure 3.

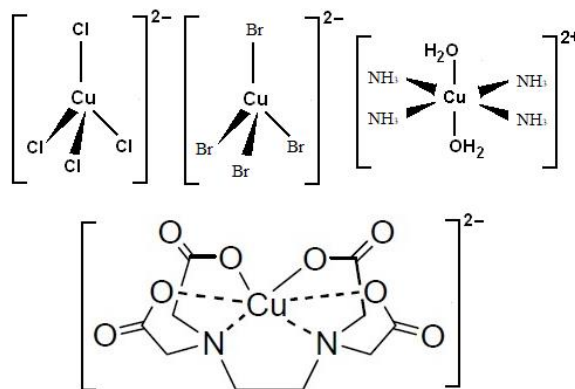


Figure 3. Copper Complexes used for EK Experiments.

These four complexing agents were selected because they readily replace some or all of the water molecules surrounding a copper ion. The radii of the Br and Cl complexes are

³¹ R. W Impey, P. A. Madden, and I. R. McDonald, *Hydration and mobility of ions in solution (The Journal of Physical Chemistry* 87, no. 25 1983), 5077.

approximately 1.42 angstroms. NH_3 creates a complex that is similar in size to the hexaaqua complex of 4.72 angstroms. Finally EDTA creates a very large and bulky complex of approximately 30 angstroms.³² In principle, the transport rates of these complexes in an EK reactor are directly proportional to their size. However counter ions (e.g., Na^+ in NaCl), pH and other substances also respond to the electric field and/or interact with the target ions, thus affecting the electro-migration process. The transport rates, therefore, must be experimentally determined. In this thesis, this was done by analyzing data collected directly from measurements of current change across the reactor (mA) and total copper concentrations sampled from the electrode compartments following a completed EK system run.

1.3. Thesis Goals and Objectives

The goal of this thesis is to assess whether EK remediation could be a viable remediation technology for heavy metal contamination similar to concentrations seen in the shallow aquifer of Butte, MT. EK remediation, although relatively understudied, could be a key to the type of *in-situ* remediation that Butte, MT needs. Before further research can be conducted, there needs to be a foundation for replicable experiments and laboratory setup. There has been some research on the effect of ammonia on electroosmotic flow and using acids to condition the electrode compartments of EK reactors. However, little research has been done on preparing the bulk contaminated solution with complexing agents prior to an EK remediation experiment. The objectives of this thesis are to: (1) develop a lab scale experiment that is replicable and produces

³² Ronald F. See, Rebecca A. Kruse, and William M. Strub. *Metal–Ligand Bond Distances in First-Row Transition Metal Coordination Compounds: Coordination Number, Oxidation State, and Specific Ligand Effects* (Inorganic Chemistry 37, no. 20, 1998), 5369.

consistent data, and (2) assess the effect of complexing agents on the electromigration transport rates of copper ions in an EK cell, by using current readings and copper concentration samples.

2. Methods and Materials

The following section describes the methods and materials that went into addressing the two objectives of this thesis. This section is divided into two sub sections. One for the experimental design of the thesis, and one for the data analysis portion of this thesis.

2.1. Experimental Design

The following sections describe the different elements of design that went in the experiments of this thesis, such as the design of the reactors, the composition of the test soil used, the aqueous solutions and titrations, quality assurance and quality control experiments, the decontamination protocol, and sampling regiment.

2.1.1. Reactor Design

Four identical small-scale reactors were constructed. Each reactor was built to the same measurements using commonly accessible power tools, and therefore the lengths and masses of each reactor vary somewhat, but not significantly. Figure 4 is a diagram of the reactor design.

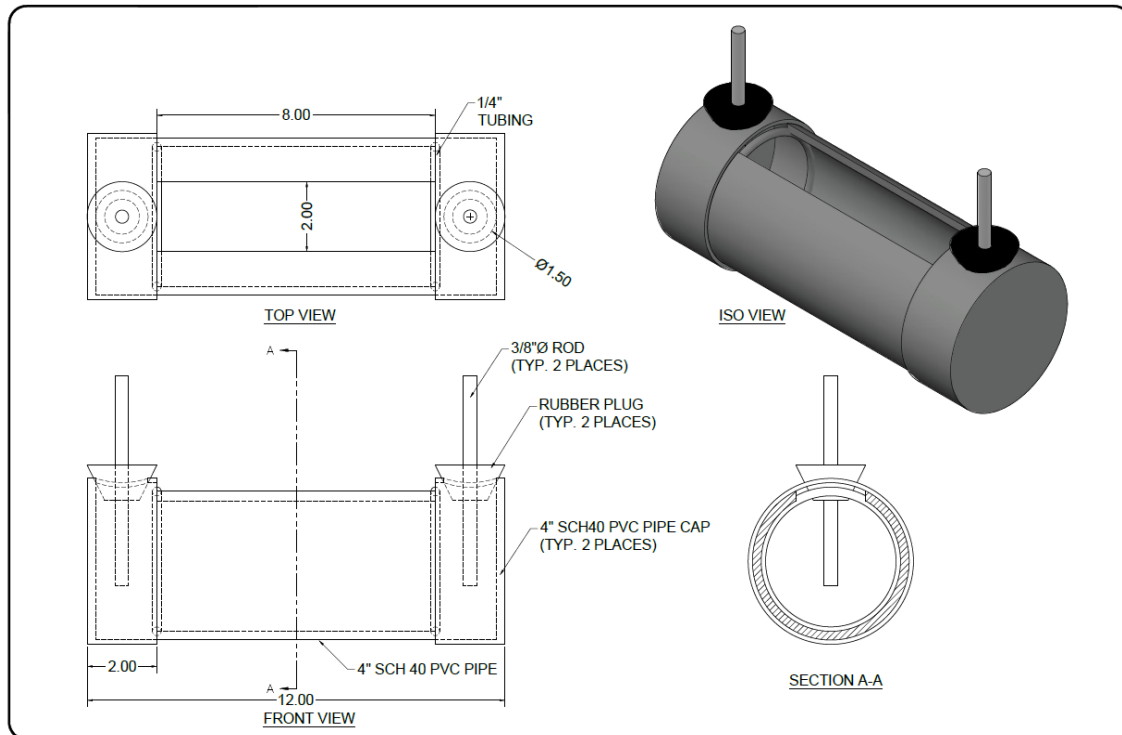


Figure 4. EK Reactor Blueprint.

The reactors were designed to exemplify one dimensional flow through a groundwater system under EK conditions. Each reactor was constructed out of a 0.3048 m (1 ft) length of 4 in Schedule 40 PVC pipe. The outside diameter of the reactors was 0.1143 m (4 in) and the inside diameter was 0.099 m (3.89 in). An approximately 4.5 cm lateral slice was removed from the PVC pipe, to allow for soil loading. Each end of the reactor was capped with a 4 in PVC cap, primed and glued. Silicone calk was then applied to all inside and outside joints to further seal the reactor. Finally, a 0.044-m (1.75-in) diameter hole was drilled into each end cap to later serve as the housing for the electrodes.

The reactor was then divided into three compartments: the positive electrode compartment, the negative electrode compartment, and the soil chamber. The electrode compartments were located at the ends of the reactors, from the end caps to the edges of the reactor. These compartments did not contain any soil. The soil chamber was the volume of space

in the reactor between the end caps. It is in this space that the soil is loaded and compacted. The electrode compartments and soil chambers are separated by a permeable barrier created by tightly wound cheesecloth. Cheesecloth was wound around semi-rigid polyvinyl tubing, which created disks that could then be inserted into the chamber, prior to loading with soil, and placed at the start of the end cap. This method was suitable for preventing soil from entering the electrode chamber and created a barrier between the electrode compartments and the soil chamber. A photo of the cheesecloth barriers is included below in figure 5, with the rigid tubing on the left, and the final wrapped tubing on right.



Figure 5. Permeable Barriers used to Separate Electrode Compartments from Soil.

The total volume of the electrode compartments was 353 cm^3 and the total volume of the soil chambers was 2020 cm^3 . The volume of the permeable barrier was neglected. Consistent compartment volumes were maintained between experiments by ensuring that the permeable barrier was seated in the same location, against the end caps, every experiment. Size 7 rubber stoppers with one center hole were inserted into the top hole of the electrode compartment and were used to house the one eighth-inch stainless steel electrodes. The electrodes were cut from a store-bought stainless-steel dowel and cut approximately 15-cm in length. Prior to each

experiment, each electrode was polished with sandpaper to a high shine, to remove any contamination from a previous experiment, or to remove the initial grease from the manufacturer. Higher end material such as carbon, or titanium are often chosen for EK experiments because they are more resistant to corrosion than steel. However, stainless steel electrodes were chosen for this experiment on idea that they would no degrade significantly over the 48 hour course of the experiment, and because they were affordable, easily obtained at a local hardware store, and likely implemented in a real-world project.

2.1.2. Experimental sand medium

An artificial sand medium was prepared in order to maintain accurate and comparable results between experiments and to control for any effect the soil might have on the transportation rates. Soil characteristics, such as porosity, tortuosity, conductivity, and many others, can affect how an electrokinetic system functions.³³ This thesis is concerned with how ion transport rates change with alterations to the hydrated radius, and therefore any effects from soil characteristics need to be controlled. A natural soil would introduce too many uncertainties into the experiments. This is because a natural soil might contain trace metals, specifically copper, that could leach into solution, and affect the mass balance of the experiment, therefore introducing a high bias to the results. Conversely, a natural soil may also act as a copper sink during the experiment, thereby introducing a low bias to the results. In addition, the heterogeneity of a natural soil makes it difficult to maintain consistent porosity, hydraulic conductivity, and density between experiments. For this reason, an artificial soil medium was used for all the experiments.

³³ Gennady Denisov, R. Edwin Hicks, and Ronald F. Probstein, *On the kinetics of charged contaminant removal from soils using electric fields* (Journal of colloid and interface science 178, no. 1, 1996), 310.

The test soil medium was 90% coarse quartz sand, 10% kaolin clay, by weight. This ratio was simplified from different research that used a similar ratio of sand and clay for an artificial soil medium.^{34,35} The coarse quartz sand used for the experiments came from a 50-lb bag of well construction sand. This sand is used to fill the annular space between a well screen and a borehole. It is made out of quartz sand that has been crushed, washed and screened to 0.5 mm. This sand is well suited for a control medium because it has been prewashed to remove impurities, and because quartz is a stable, hard, and inert mineral, meaning that it does not interact with any of the electrochemical reagents that went on inside the reactor. Kaolin clay was selected for similar reasons. Kaolin clay has a particle size range between 25 to 35 micrometers. Bulk batches of the soil medium were prepared in a 5 gallon bucket and mechanically mixed using a clean, plastic drill attachment. The medium was stored in the same 5-gallon bucket and sealed with a lid to prevent any laboratory contamination from coming in contact with the unused medium.

2.1.3. Reactor Loading

Each reactor was loaded systematically with the soil medium prior to each experiment. Empty reactors were massed before and after being loaded, to determine the mass of soil packed into the soil chamber. Soil medium was added to the soil chamber in approximately 250-mL lifts. Each lift was then tamped down using a handheld 1-in diameter wooden dowel. Both 250-mL soil cup and dowel were periodically cleaned and stored with the soil medium. Compaction was

³⁴ Susheel K. Puppala, Akram N. Alshwabkeh, Yalcin B. Acar, Robert J. Gale, and Mark Bricka. *Enhanced electrokinetic remediation of high sorption capacity soil*, (Journal of Hazardous Materials 55, no. 1-3 1997, 204.

³⁵ Lizhu Yuan, Xingjian Xu, Haiyan Li, Quanying Wang, Nana Wang, and Hongwen Yu, *The influence of macroelements on energy consumption during periodic power electrokinetic remediation of heavy metals contaminated black soil* (Electrochimica Acta 235 2017). 606.

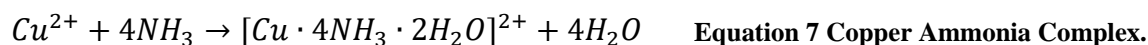
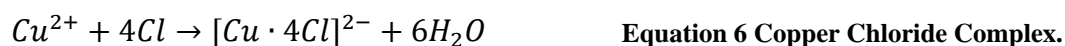
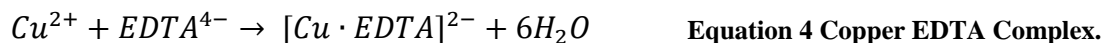
deemed to be complete when the soil had a particular resistance to it, however no analytical method was available to ensure that the compaction was maintained between experiments. The cylindrical design of the reactors made it difficult to utilize a more standardized approach, such as dropping a known mass from a set height a number of times. Future experiments may want to consider foregoing the convenience of a PVC pipe design and instead building rectangular reactors that would allow for more consistent loading procedures.

2.1.4. Solution Preparation

A total of five solutions were used in the experiments of this thesis, each consisting of the baseline solution either alone or combined with one of the four complexing agents. A copper concentration of 716 mg/L was used as the baseline solution for every experiment conducted for this thesis. This concentration is based on the copper concentration of a sample taken from the monitoring well GS-19D. Monitoring well GS-19D is screened in the Parrot Tailings in Butte, MT. As mentioned in the introduction, this area was been heavily impacted by mining activities in the early century, resulting in groundwater metal concentrations high in copper, zinc, and iron. The metal concentrations of the well are similar to many sites affected by acid rock drainage and mining activity, and they are ideal for electrokinetic remediation. A solution concentration of 716 mg/L was achieved by massing 2.80 grams of copper sulfate pentahydrate ($\text{CuSO}_4 \cdot 5\text{H}_2\text{O}$) per liter of deionized water. A confirmation sample using this mass of $\text{CuSO}_4 \cdot 5\text{H}_2\text{O}$ was analyzed using EPA Method E200.2 inductively coupled plasma-mass spectrometry (ICP-MS). This was done to verify that the laboratory stock salt was correctly hydrated. The ICP results for this solution were 737 mg/L which indicated that the stock salt had slightly dehydrated and contained a higher proportion of copper per mass salt. This concentration of 2.80 grams $\text{CuSO}_4 \cdot 5\text{H}_2\text{O}$ per liter deionized water was still maintained over the course of the experiments,

but the actual copper concentration likely ranged from 716 mg/L to 737 mg/L. This solution had an initial pH of 2.5.

The Ethylenediaminetetraacetic (EDTA) copper sulfate solution was prepared by dissolving 0.720-grams of EDTA into the baseline solution. The mass of EDTA and volume of HCl, HBr, and EDTA are based on the stoichiometric relationships given below:



Following titrations to determine the molarity of the laboratory stock solution, the HCl, HBr, and NH₃ solutions were prepared by adding 5 ml of HCl, HBr, or NH₃ to the baseline solution. These volumes were also based on the stoichiometric relationships given above and were rounded up to 5 ml to allow for more practical measurements, and to ensure that the solution was properly complexed. Solutions were prepared immediately before each reactor experiment, to avoid any volatilization or cross contamination that could potentially happen if the solutions were produced in bulk and stored long-term.

2.1.5. Reactor experiments

After the reactors were loaded with soil, massed, and the experimental solution was prepared, the experiment was ready to begin. The reactors were placed onto small wooden stands

that would keep the cylindrical reactors in place and would insulate them from any errant electrical grounds. The power source and data program, which will be discussed in more detail in a later section, allowed for two reactors to be ran at a time. The experimental solution was slowly poured into the loaded reactors at the two openings in the electrode compartments. The solution was poured slowly to prevent any of the soil from collapsing the cheesecloth barriers and spilling soil into the electrode compartments. A liter of solution was poured into the reactor, causing a water level rise of 7 cm above the bottom of the reactor. This left 2 cm of soil above the water level that was well saturated due to capillary action but prevented any surface pooling of solution that could short circuit the reactor. After adding the solution, the reactors sat for 5 minutes to allow the solution level to fully equilibrate. Following this, the polished steel electrodes were inserted into the number 7 rubber stoppers, and the rubber stoppers were inserted into the holes above the electrode compartments. Alligator clips were wired into the power source and data program and were clipped onto the portion of the electrodes that protruded out of the top of the reactor. Prior to this, the power source was confirmed to be powered off, to minimize any risk of electric shock. Once connected, the power source and data recording program were turned on, and the reactors were ran at a voltage gradient of 30 volts for a period of 48 hrs. Figure 6 is a photo of the laboratory setup and reactors.



Figure 6. Laboratory Experiment Setup and Reactors.

Figure 6 shows the laboratory setup. Shown near the bottom are reactor R1 and R3. Right of the laptop, is the National Instruments data acquisition (DAQ) module, and relay board. Above this is the power source, used to maintain a constant potential of 30-volts across the reactors during the experiments.

2.1.6. Decontamination

Prior to running the reactor experiments, each reactor and its components were cleaned to prevent any cross contamination from occurring between experiments. Each reactor, the electrode compartment tubing, and the rubber stoppers used to hold the electrodes, were rinsed and scrubbed under warm tap water and Alconox detergent. Following this, the reactors and components were soaked, rinsed, and scrubbed in a 10% HCl solution, before a final rinse with

DI water. They were then air dried, before being returned to the wooden frames that house and insulate the reactors. While the reactors and their components were soaking in the HCl solution, the work bench in the laboratory was prepped for the experiment. The bench and other work areas were cleared of any loose or unnecessary equipment, and then wiped down using a diluted Alconox solution and paper towels. Electrodes were polished prior to each experiment by sanding them with a medium grit sandpaper. This process removed any contamination from previous experiments, contamination that may have settled on the rods in storage, or the layer of factory anti-corrosion grease that initially coated each rod. The reactors were also periodically inspected for leaks and repaired if necessary.

A blank reactor was used to verify that the decontamination process was adequate at preventing cross contamination in the laboratory. The blank reactor was prepared following the same methods that the experimental reactors are prepared. In brief, a reactor was rinsed, and decontaminated after an EK experiment, loaded with test soil, filled with DI water and set on the laboratory work bench. For experimental reactors, two reactors were rinsed, decontaminated, loaded and filled with a copper experimental solution. The laboratory blank was set next to these two reactors and remained there for the duration of the 48-hr experiment. Once the experiment was complete, and the experimental samples were taken, the blank reactor was sampled in the same fashion as the experimental samples. Results for the blank reactor are included with the results for the experimental samples.

2.1.7. Waste Management

This thesis involved experiments that produced significant amounts of waste copper salts, as well as caustic solutions resulting from the addition of HCl, HBr, EDTA, or NH₃. More than twenty-five EK experiments and trials, and numerous minor tests and titrations were conducted

over the course of this thesis. A waste management protocol was designed in order to avoid contributing a significant heavy metal load of the local wastewater treatment facility, and to prevent damage to the laboratory sewage pipes. Following each experiment, the soil and solutions in the reactors and any associated equipment were spread out into a large plastic basin (22-in by 16-in). Any residual soil and solution remaining in the equipment was then further rinsed off with water into a 5-gallon bucket. The basin and bucket were stored on a ledge in the laboratory near a window, where the sunlight promoted high evaporation rates. A space heater was also used periodically during the winter months to increase evaporation rates and keep up with the experimental waste production rates. When the basin or bucket were dry, the soil waste was double-bagged and disposed of at the local landfill.

2.2. Experimental Data and Analysis

The following sections describe the different types of data acquired during this thesis, and how that data was analyzed.

2.2.1. In-situ current monitoring

Figure 7 is a wire diagram of the laboratory set up that was used to collect current (mA) readings in the reactors. For clarity, only one reactor wiring is shown in the diagram; however, the actual direct current power source had two channels, allowing for two reactors to be ran independently.

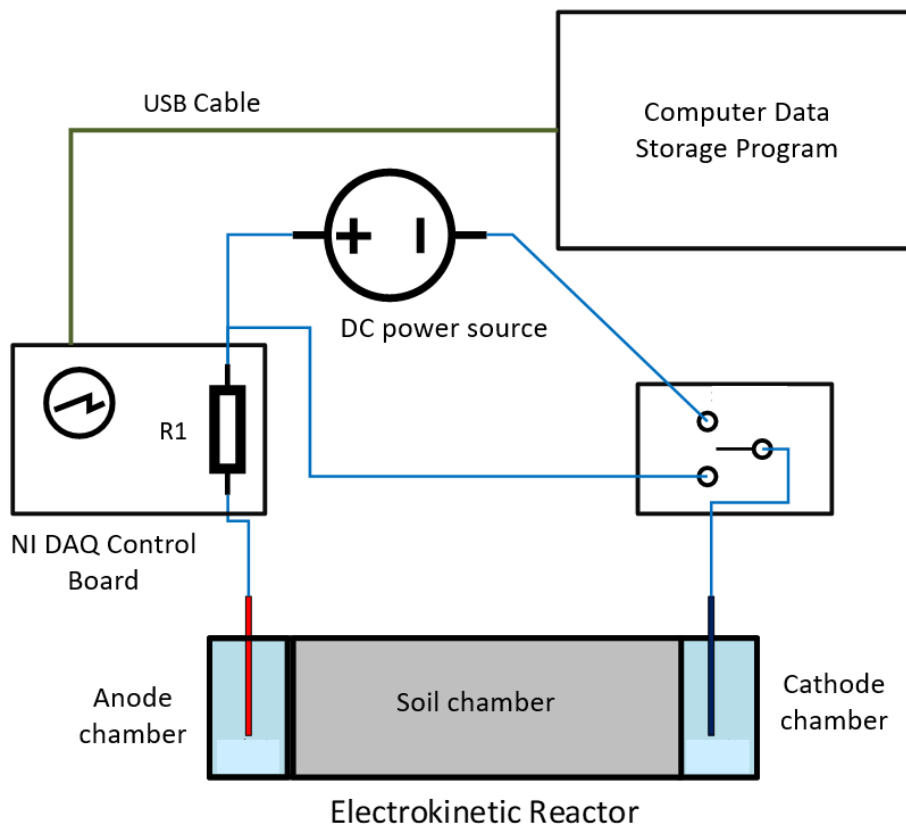


Figure 7. Wire Diagram of EK experiments.

The power source and reactor were wired into a single pole double throw (SPDT2) relay that could switch between energizing and short-circuiting of the EK reactor. This setup allowed one to de-energize the system, without the need to turn off the power source, or stop the program. Once the system was energized and the program was running, the EK remediation would proceed in the reactor. Connected in series to the positive lead of the power supply, was a 10-Ω metal film resistor (R1 in the diagram). A National Instruments DAQ module measured the minor voltage drop across the resistor. From there it would calculate the current, and record that value every minute of the experiment, using Ohm's Law:

$$v = i * R$$

Equation 8 Ohms Law.

where v is the voltage (volts), i is current (amps), and R is resistance (ohms).³⁶ The purpose of this data was to provide a means of tracking the conductivity changes inside the reactor, thereby providing a way to estimate transport velocities for target ions or ion complexes.

2.2.2. Reactor sampling

After running for 48 hrs, the reactors were de-energized. The electrodes were removed and massed. After that the reactor was also massed. The water sample in each electrode compartment was collected and analyzed for total copper concentration. The copper analysis was done by Energy Laboratories in Helena, MT using EPA Method E200.2 inductively coupled plasma-mass spectrometry (ICP-MS). Water samples were taken using a 35-ml syringe to remove approximately 90-ml of electrolyte solution from the electrode compartments. The result was approximately 90 to 100-ml of original sample volume. To minimize any bulk fluid movement during sampling, both ends of the reactor were sampled at the same time. Simultaneous sampling minimized any fluid displacement caused by the syringe insertion because the hydraulic gradient created by the displacement from one syringe was matched by the displacement on the syringe at the other end of the reactor. Once the sample collection was completed, the original sample in the cylinder was recorded. The ICP-MS analysis required a sample volume between 200 to 250-ml, so after the original sample volume was recorded, the samples were diluted with DI water up to a suitable volume. The final volume was again recorded. Following ICP-MS analysis, the original electrolyte concentrations were back calculated as follows:

³⁶ Charles K. Alexander, and Matthew no Sadiku. *Electric circuits* (Transformation 135 ,2000), 31.

$$\text{Electrode Concentration} = \frac{(\text{Dilution Concentration}) \times (\text{Dilution Volume})}{\text{Original Volume}}$$

Equation 9 Electrode Compartment Concentration.

A sample was taken from each of anode and cathode compartments, and one set of samples was submitted for each experiment, as well as a laboratory blank (a total of 11 samples).

2.2.3. Data Analysis

The purpose of the data analysis of this thesis was to help draw conclusions on the transport velocities seen in different experiments. This was done by using the minute-by-minute current recordings to calculate the ion concentration in an electrode compartment and developing a relationship for the change in ion concentrations with time. The raw data was imported into a Microsoft Excel file and sorted by experiment type for analysis. The ion concentration in an electrode compartment was calculated using the equation:

$$C = C_0 e^{ItK} \quad \text{Equation 10 Concentration Change.}$$

where C is the concentration in the electrode compartment (mg L^{-1}), C_0 is the initial concentration in the compartment (mg L^{-1}), I is the amperage reading (Amps), t is time (seconds), and K is the apparent rate constant (Amps^{-1} , seconds^{-1}). This equation was repeated as an iterative process where the concentration result (C) from the previous minute became the starting initial concentration (C_0) for current minute, using that current amperage reading. This data analysis method was developed for this thesis. The apparent rate constant, K , was selected as a curve fitting constant. This constant incorporates transport factors, such as ionic mobility, that are difficult to measure directly. This empirical equation is based off of the relationship given in equation 1, which states that as current is directly proportional to the flux density N_i of the electrolyte solution. Therefore, as the current decreases, the ionic flux decreases. The equation is based off a mathematical solution for the molecular dispersion of an instantaneous electrolyte input, or slug input. The original equation uses a known initial concentration, and a

known dispersion coefficient to approximate concentration changes over time. However, this version has been modified so that the analogous dispersion coefficient, the current, changes as the system evolves. In other words, this equation models diffusion in which the dispersion coefficient is not constant. The value of the apparent rate constant was chosen based on how closely it replicated the concentrations from the sampled ICP-MS results. By reversing the sign on the apparent rate constant, equation can be used to estimate the concentration in either electrode compartment. A negative value simulates concentrations changes in the electrode chamber that is being depleted, while a positive value simulates concentration changes in the electrode chamber that is being enriched.

The transport velocities of each type of experiment were estimated by fitting a linear equation to the concentration curve created by equation 9. The slope of this linear equation was then multiplied by the electrode compartment volume to give the mass change in mg s^{-1} .

$$Q = S \times E \qquad \text{Equation 11 Mass change per second.}$$

where Q is the mass entering the electrode compartment (mg s^{-1}), S is the slope of the linear equation ($\text{mg L}^{-1} \text{s}^{-1}$), and EC is the electrode compartment volume (L).

As the results will show, the rates of depletion and enrichment dramatically change near the 12.5 hour mark in nearly all the experiments. For this reason, the transport velocity was estimated for the 0-12.5 hour interval, the 12.5 to 48 hour interval and the overall transport velocity.

3. Results

The following section is divided into two separate sections. One section is devoted to the experimental results, such as the mass tracking of the reactors, and the ICP sample results. The second section is devoted to the current readings and the transport velocities determined from the data analysis.

3.1. Experimental Results

This section describes the physical results collected from the experiments, including the mass change of the reactors, the mass losses and gains to the experimental electrodes after the experiments. As stated in the results, the masses of soil and solution were carefully tracked during the experiments. The soil mass table included in Appendix A, provides a summary of the mass changes during the electrokinetic experiments. This table shows that over the 17 EK experiments, the average mass of soil loaded into the reactor was 2.35 kg. The standard deviation from this average was 0.06 kg, with minimum and maximum soil masses at 2.24 kg and 2.47 kg, respectively, showing that a consistent mass reactor was maintained throughout the course of the experiments. The table also shows that the average mass of solution lost to evaporation was 0.08 kg, with standard deviation of 0.02 kg. The minimum and maximum evaporation masses were 0.05 kg and 0.10 kg, respectively. Electrode masses were also tracked pre and post experiment, seen in the figures below.

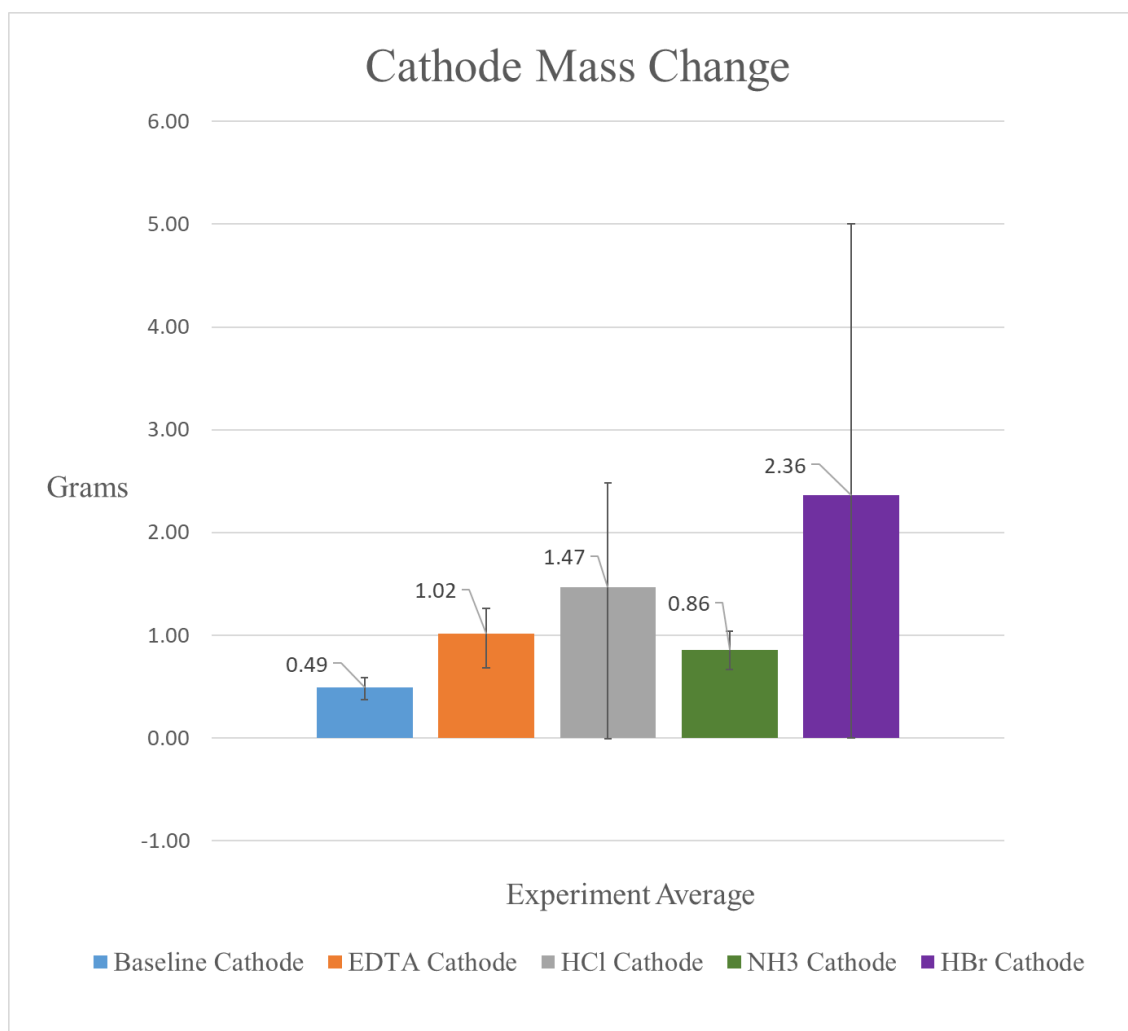


Figure 8. Cathode Mass Change during 48 hour experiments.

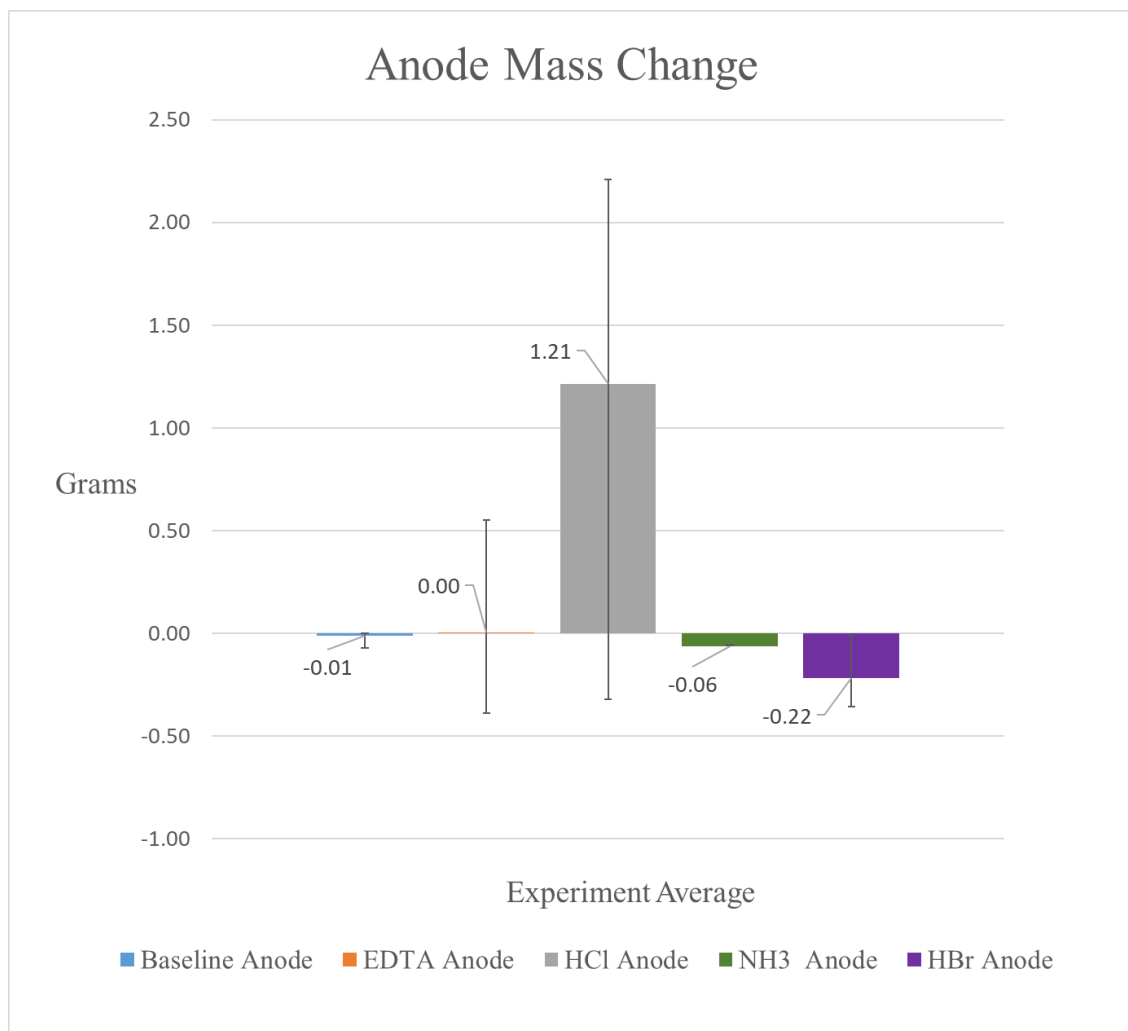


Figure 9. Anode Mass Change during 48 hour experiments.

Figures 8 and 9 show the average mass changes on the cathodes and anodes respectively over the course of the experiments. Negative values represent instances where the electrode lost mass over the course of the experiment, and positive values correspond to mass gains on the electrode. Mass losses on the electrode are attributed to oxidation and acidic corrosion of metals off of the stainless-steel electrode. Mass gains are attributed to reduction and precipitation of metals onto the electrode. Even in terms of the same test solution, the results show a wide and inconsistent range of mass losses at the cathode ranging from 5 g in an HBr trial to a mass gain of 0.01 g in an HCl trial. Likewise, the results show a wide range of mass gains on the electrode

with a maximum loss of 2.21 g in an HCl trial, and a maximum mass gain of 0.39 g in an EDTA trial. Figure 10 below is a photo of a set of electrodes following an EDTA reactor experiment.



Figure 10. Photo of electrodes following Baseline Experiments.

The left portion of the figure above shows two pairs of dried electrodes following two Baseline experiments. The black and blue electrodes correspond to the cathodes of reactors R1 and R3. The red electrodes correspond to the anodes of R1 and R3. The cathodes showed visual evidence of potential reducing conditions in the red-brown particulate adhered to the electrode surface. While the anodes showed evidence of oxidizing conditions in the blue-black particulate adhered to the electrode. The reducing and oxidizing conditions observed would lead one to think that the cathode would show mass gains while the anode would show mass losses. However, this was not seen in the mass results. It may be because the electrodes were not properly massed after the experiments. When the electrodes were removed from the reactor, they were wet, and any redox products were expanded and loosely adhered to the electrode, as seen

on the electrode in the right of Figure 10. Before being massed, they were air dried, but it is possible that mass flaked off during this process and was not accounted for during the mass balance.

The electrodes developed oxidized and reduced particulate following each experiment. However, only the EDTA experiments resulted in actual solid copper electroplating onto the electrodes, as seen in Figure 11 below.



Figure 11. Copper Plating on Positive EDTA Electrode after polishing.

Reduced copper was not observed following any of the other experiments. This is interesting considering EDTA, HCl and HBr all produce complexes with 2^- charges.

Following each experiment, both electrode compartments were sampled according to the process outlined in the section 2.2.2 of this thesis. As stated, one set of samples from each type of experiment was submitted to Energy Laboratories and analyses for total copper. The analysis results are included in Table I below.

Table I. Total Copper Concentration ICP Results.

Sample ID	Date	ICP result Cu, mg/L	Volume Sampled (ml)	Final Dilution (ml)	Corrected mg/L
Baseline Anode	1/31/2019	729	102	210	1500.9
Baseline Cathode	1/31/2019	69.6	96	220	159.5
HCl Anode	2/28/2019	627	120	230	1201.8
HCl Cathode	2/28/2019	219	110	230	457.9
EDTA Anode	2/21/2019	3.63	96	210	7.9
EDTA Cathode	2/21/2019	405	104	201	782.7
HBr Anode	3/7/2019	331	104	226	719.3
HBr Cathode	3/7/2019	52.3	88	212	126.0
NH ₃ Anode	3/15/2019	340	118	238	685.8
NH ₃ Cathode	3/15/2019	285	110	220	570.0
Reactor Blank	3/12/2019	0.053	250	250	0.1

Table I shows the copper concentration results from ICP analysis and corrected for dilutions. As stated in in methods section, the initial copper concentration in all the experiments was 716 mg/L. Copper concentrations for Baseline experiments was seen to increase in the anode compartment and decrease in the cathode compartment, following what was expected given the initial 2+ charge due to the copper hexahydrate ion. The Baseline experiment showed the highest level of copper enrichment across all the experiments. The HCl and HBr results showed a concentration increase in the anode compartment and a concentration decrease in the cathode compartment. These results are interesting, given that the initial 2- charge due to the complexes created by Cl⁻ and Br⁻ were expected to show enriched concentrations in the cathode

compartment rather than the anode compartment. The EDTA results show a concentration increase in in the cathode, as predicted by the initial complex charge of 2+, the EDTA anode concentration also showed the greatest depletion of copper from the original concentration, across all the experiments. The results from the NH₃ experiments showed depletion in both reactor compartments. The reactor blank results showed a trace amount of copper contamination. However, this low-level detection was not considered to impart any bias on the overall sample results, as all other concentrations were well over ten times the blank sample results.

Given the initial copper concentration of 716 mg/L and the electrode compartment volume of 264.25 ml, the mass of copper in the electrode compartment is 189.2 mg, initially. Figure 12 and 13 show how the different experiments caused the initial concentration to enrich or deplete respectively. Percent enrichment and depletion were calculated using the percent change formula.

$$\text{Percent Change} = \frac{ABS(M_i - M_f)}{M_i} \times 100 \quad \text{Equation 12 Percent Change.}$$

where M_i is the initial mass of copper in the electrode compartment (189.2 mg), and M_f is the final mass of copper in the electrode compartment.

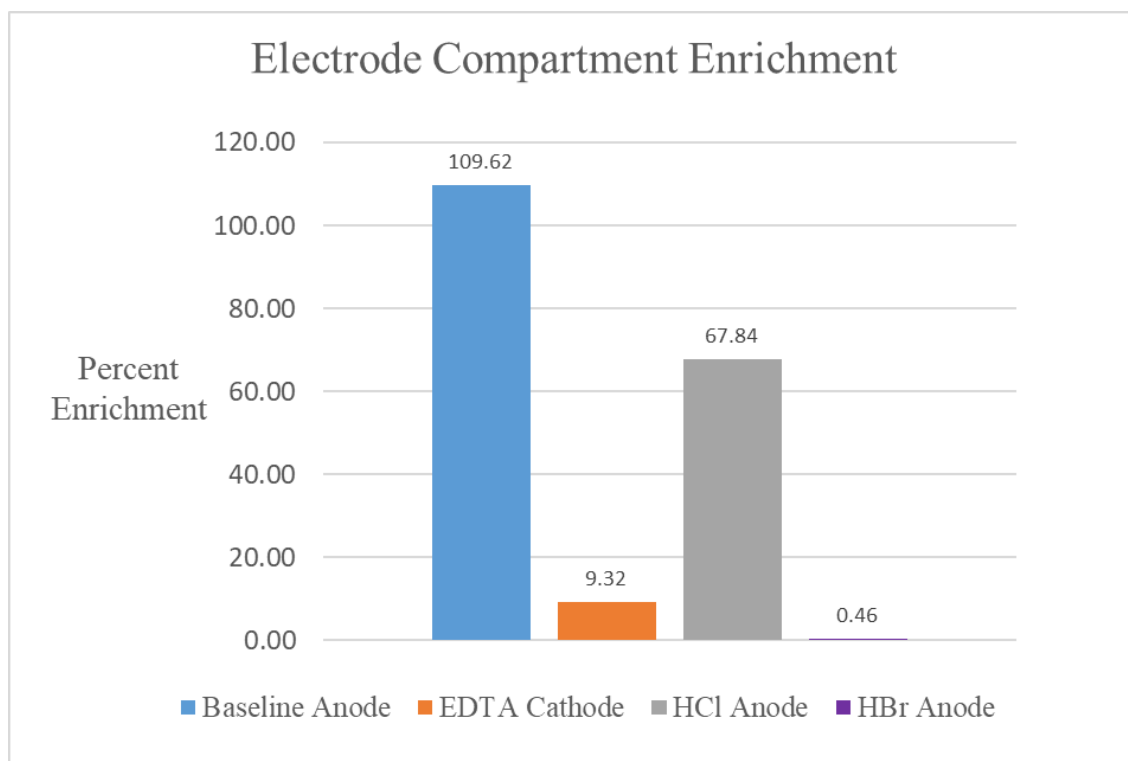


Figure 12. Electrode compartment percent enrichment.

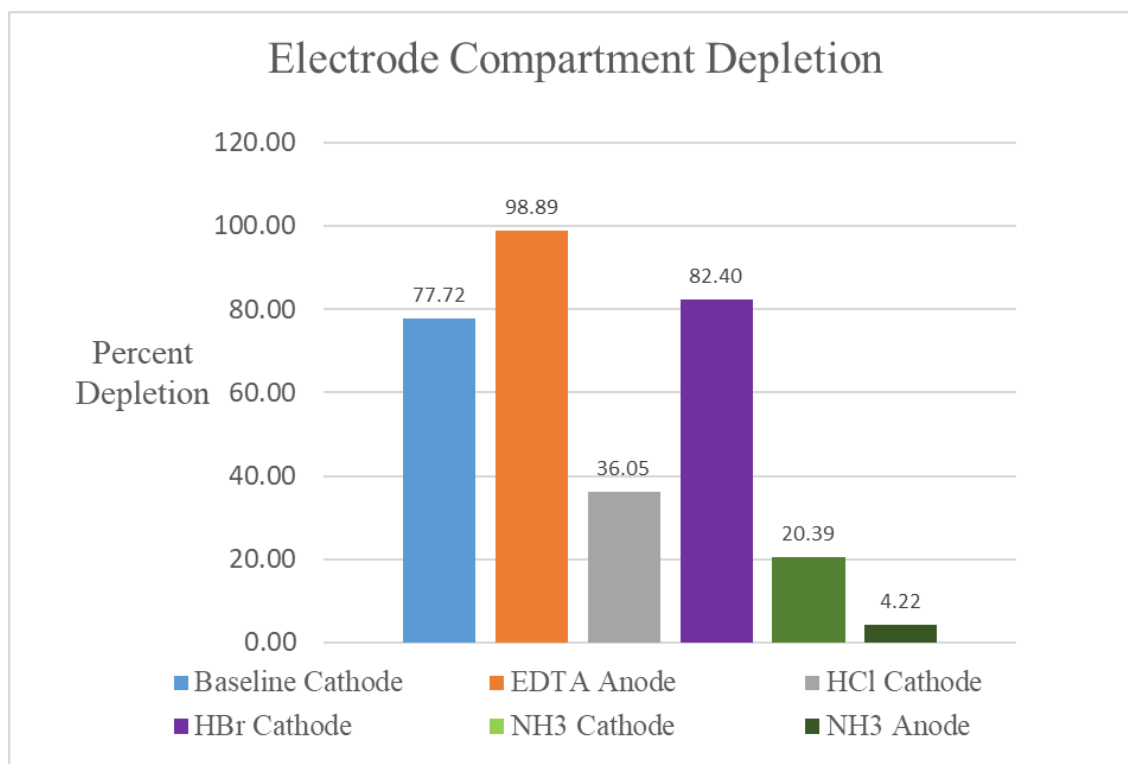


Figure 13. Electrode Compartment percent depletion.

Figure 12 shows that the Baseline experiments produced the highest factor of enrichment, followed by the HCl, EDTA and HBr experiments. However, it is important to note that copper electroplating was observed during the EDTA experiments. This mass of copper was not accounted for during the ICP-MS sampling, and therefore the enrichment values for EDTA have a low bias. Figure 13 shows that EDTA was the most successful complexing agent in depleting the electrode compartment, followed by the HBr and Baseline experiments, which produced similar depletion factors. Trailing the baseline experiments are the HCl and NH₃ experiments. Only depletion was seen in the NH₃ experiments, which may be a sign that the pH fronts caused by electrolysis at the electrodes causing the complexes to become insoluble and precipitate out of solution. Precipitation was a major sink of copper mass throughout the experiments. While it was difficult to quantify pH changes during the experiments, it is likely that the cathode created basic conditions which inhibited the transport of copper into the compartment and caused copper to fall out of solution. Figure 14 below is a bar graph showing the overall percentage of copper inside the EK reactors following the 48 hr experiments.

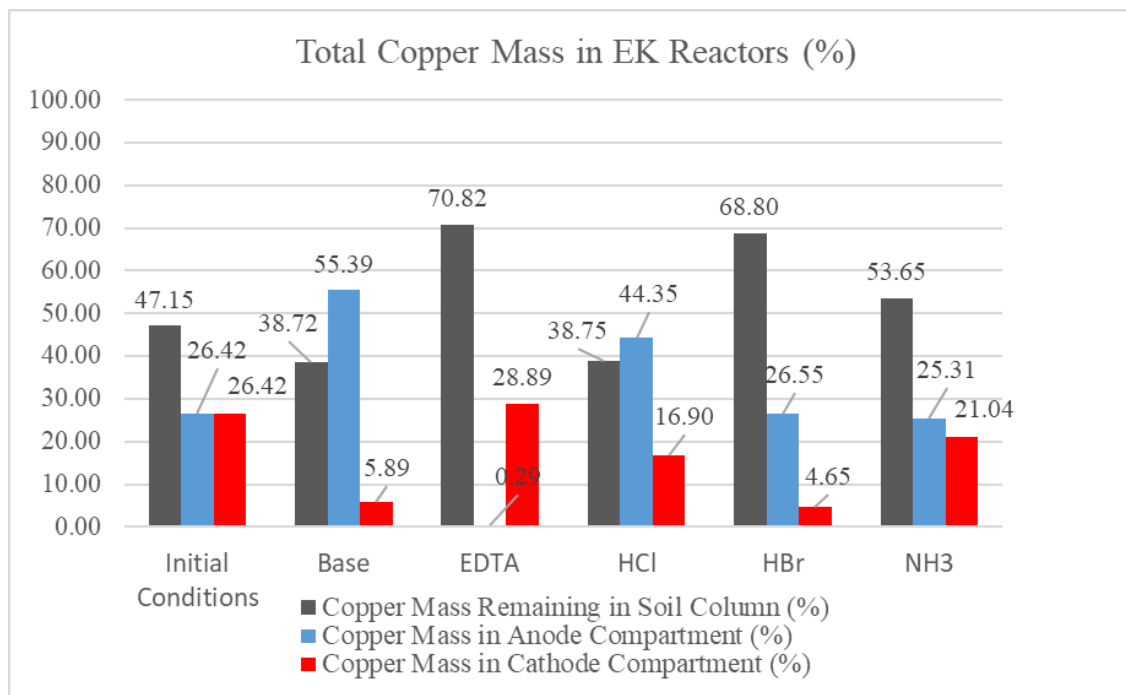


Figure 14. Copper Mass in the Electrode Chambers and soil column.

This bar graph shows that across all five experiment types, a large portion of the copper mass remained in the soil column. The graph also shows the initial distribution of copper inside the reactors before the experiments. These values are consistent across the experiments because the same copper concentration was used for each experiment. Without quantitative pH data, it is difficult to determine if this copper mass in the soil column existed as precipitate, or if it was still soluble.

3.2. Data Analysis Results

The following section is divided into four sections for (1) the current (mA) results recorded over the course of the EK experiments, (2) and (3) the enrichment and depletion calculated in the electrode compartments, and (4) the calculated transport rates for each type of experiment. Transport rates are estimated for both the depleted and enriched electrode compartments. The depleted electrode compartment is the side of the reactor that has the same charge as the copper ions or complex ions, and therefore repels the ions, causing a reduction in concentration. The

enriched compartment is the side of the electrode with an opposite charge, which displays an increase in concentration.

3.2.1. Current Measurements

Figures 15 through 19, given below, are graphs of the current readings over time. It should be noted that the current readings, plotted on the Y-axis are at different scales across the figures. The HCl and HBr experiments produced initial currents around 200 milli amps (mA), while the others were in the range of 30 to 60 mA. A great deal of clarity is lost if they are plotted on the same scale. Figure 15 is a graph of the current data taken from the Baseline experiments. This figure shows initial current readings between 20 and 30 milliamps (mA), and a decrease of current to around 5 mA as the system progressed. Around the 500-minute point in these experiments, the current decreased much more rapidly. Figure 16 is a graph of the EDTA experiment current readings. This graph shows readings of higher initial current, before decreasing to around 12 to 18 mA at the end of the experiment. Similar to the Baseline experiments, the EDTA experiments also show a gradual current decrease during the first 1000 minutes of the experiments, before more rapidly dropping off. Figure 17 and 18 are graphs of the HCl and HBr experiment current readings. The initial current was significantly higher in these experiments, at 140 to 200 mA. The HCl and HBr current readings all declined quasi-exponentially over the course of 48 hours. Finally, figure 19 shows the NH₃ experiments in which the initial current readings were much lower compared to the other experiments. This figure shows rapid drop in current at the 500-minute mark, like the Baseline experiments, although less pronounced.

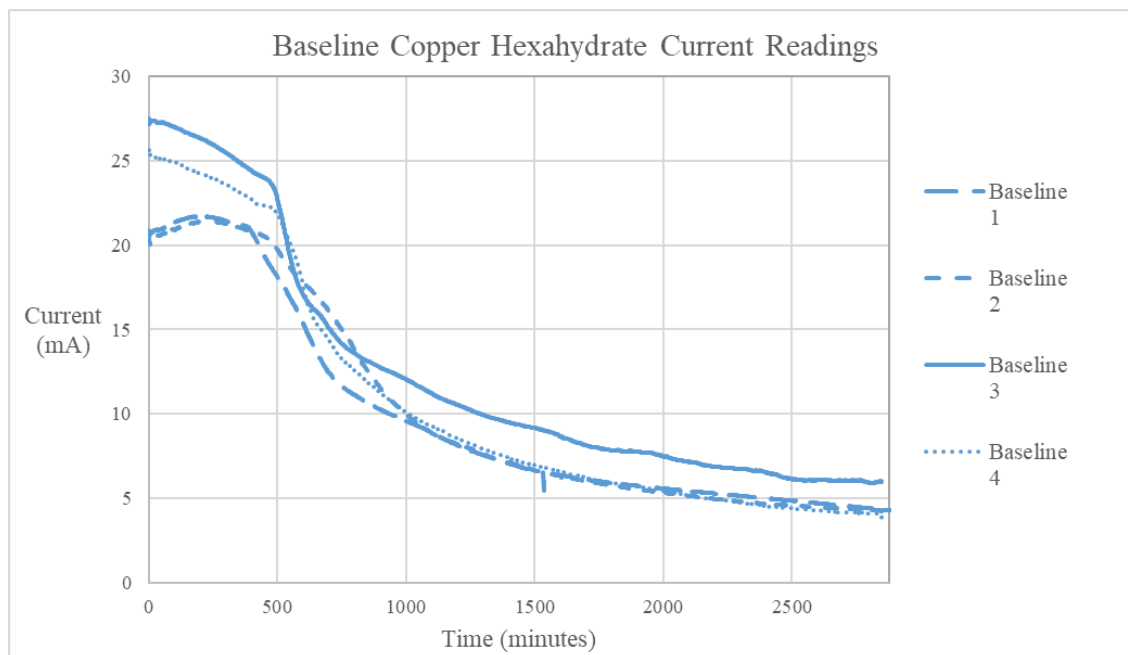


Figure 15. Copper Hexahydrate Current Readings.

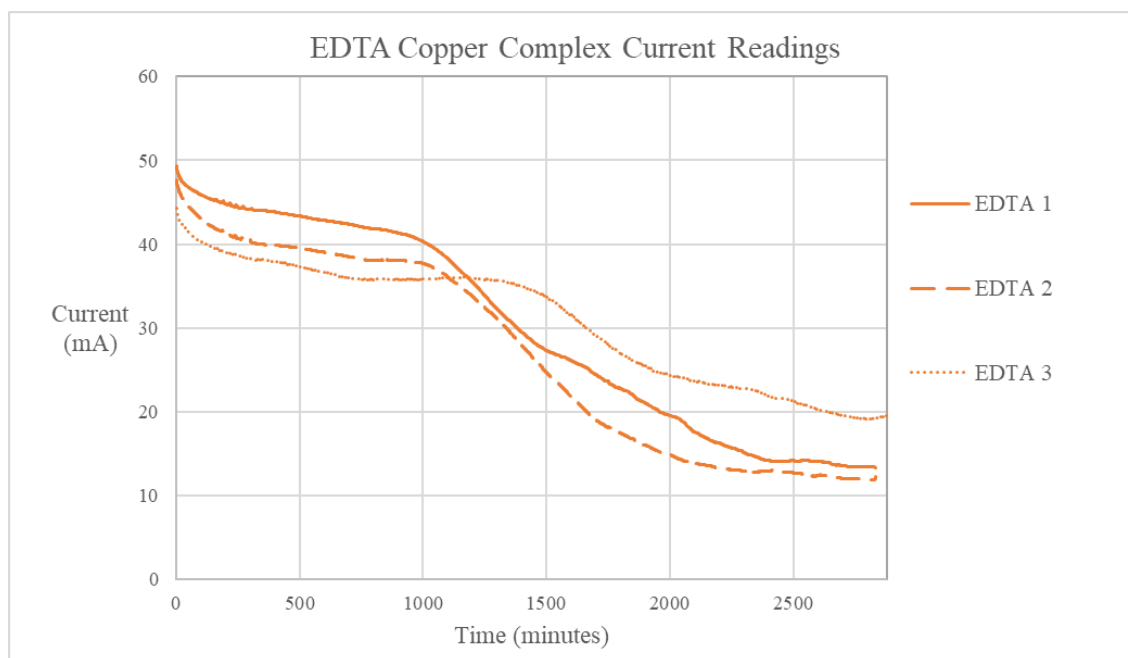


Figure 16. Copper-EDTA Current Readings.

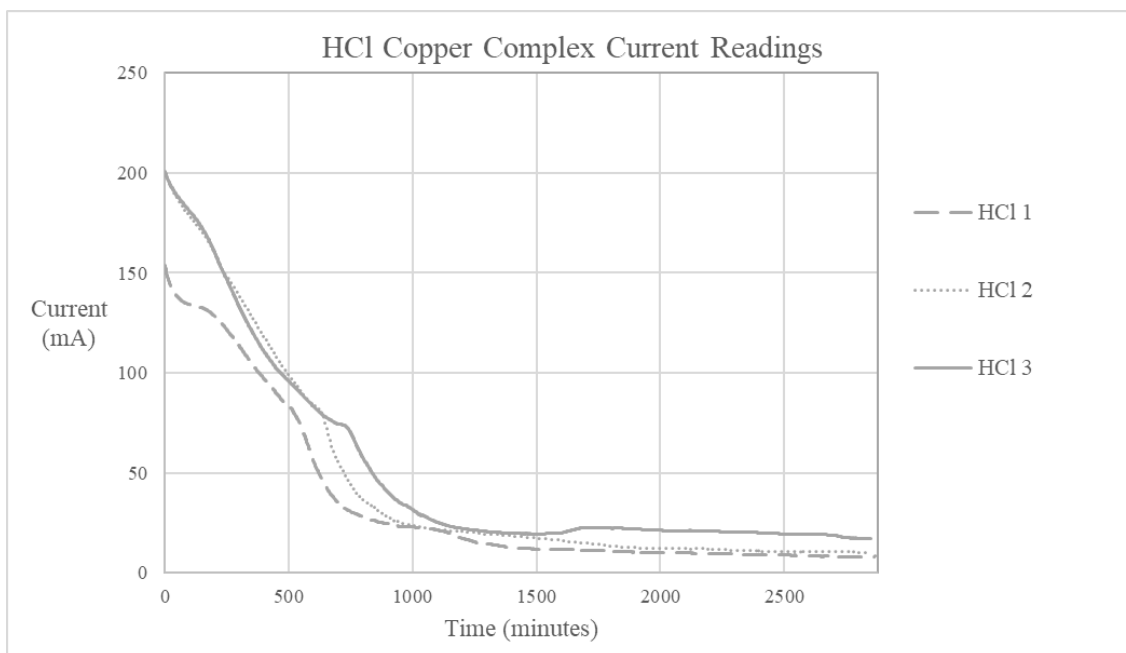


Figure 17. Copper-HCl Current Readings.

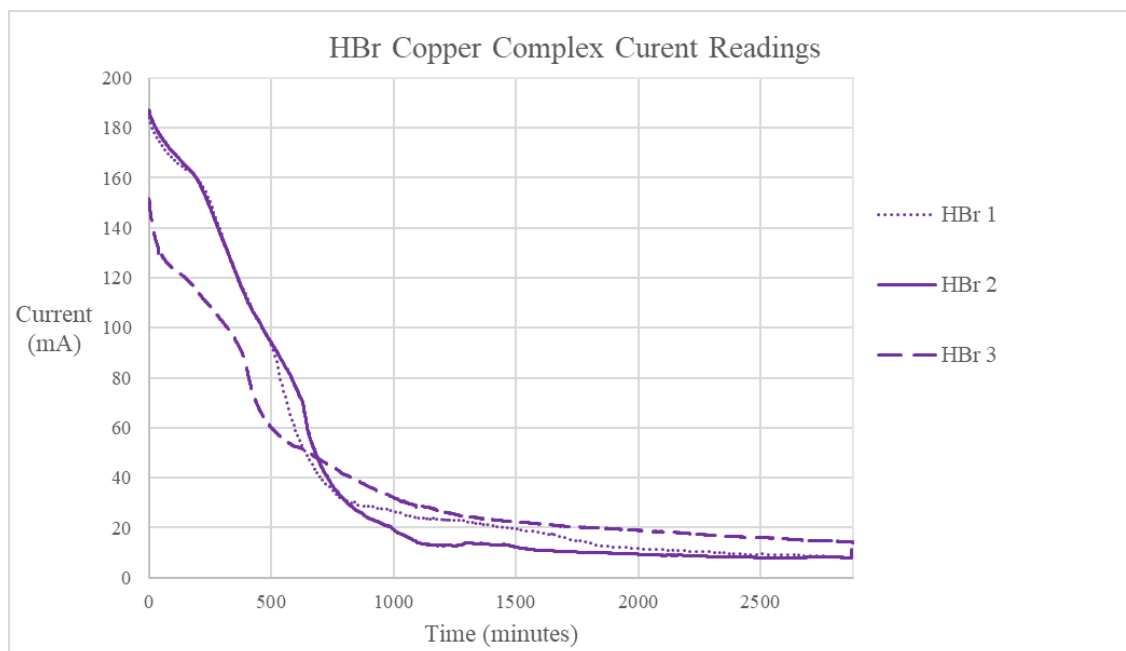


Figure 18. Copper-HBr Current Readings.

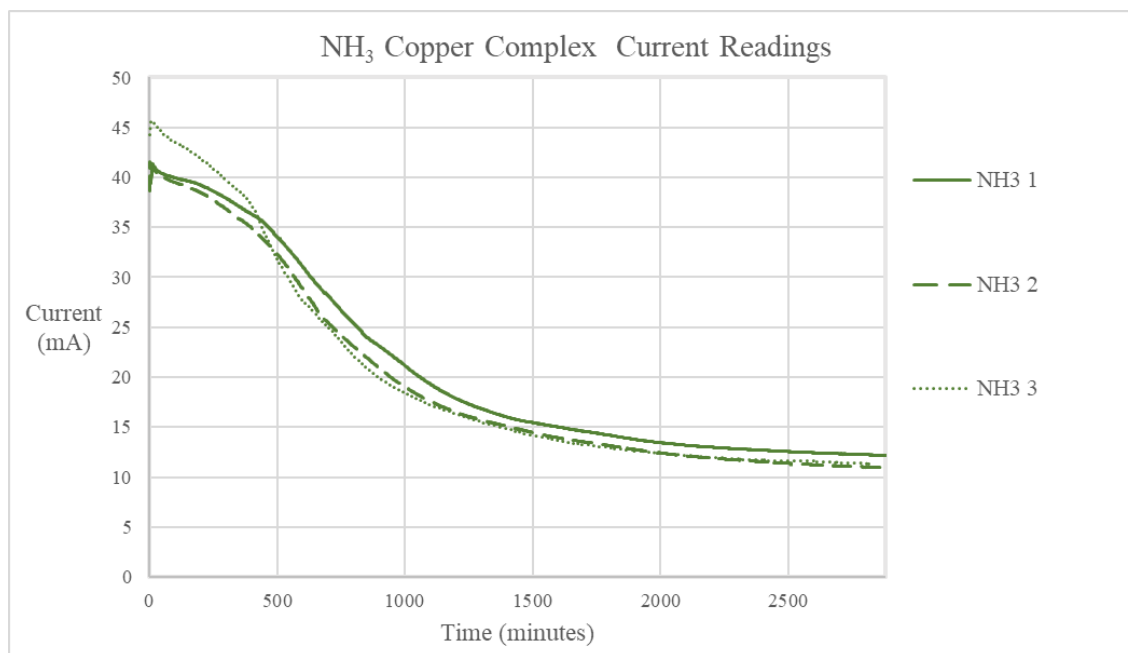


Figure 19. Copper-NH₃ Current Readings.

3.2.2. Electrode Compartment Depletion

The current data was then analyzed using the equation 9 to estimate the mass transportation out (depletion) of the electrode compartments. Figure 20 shows the calculated depletion of copper in the electrode compartments, as well as the concentrations measured at the end of the experiments and analyzed using ICP-MS, marked with “X’s” at the 48 hr (2880 minute) mark.

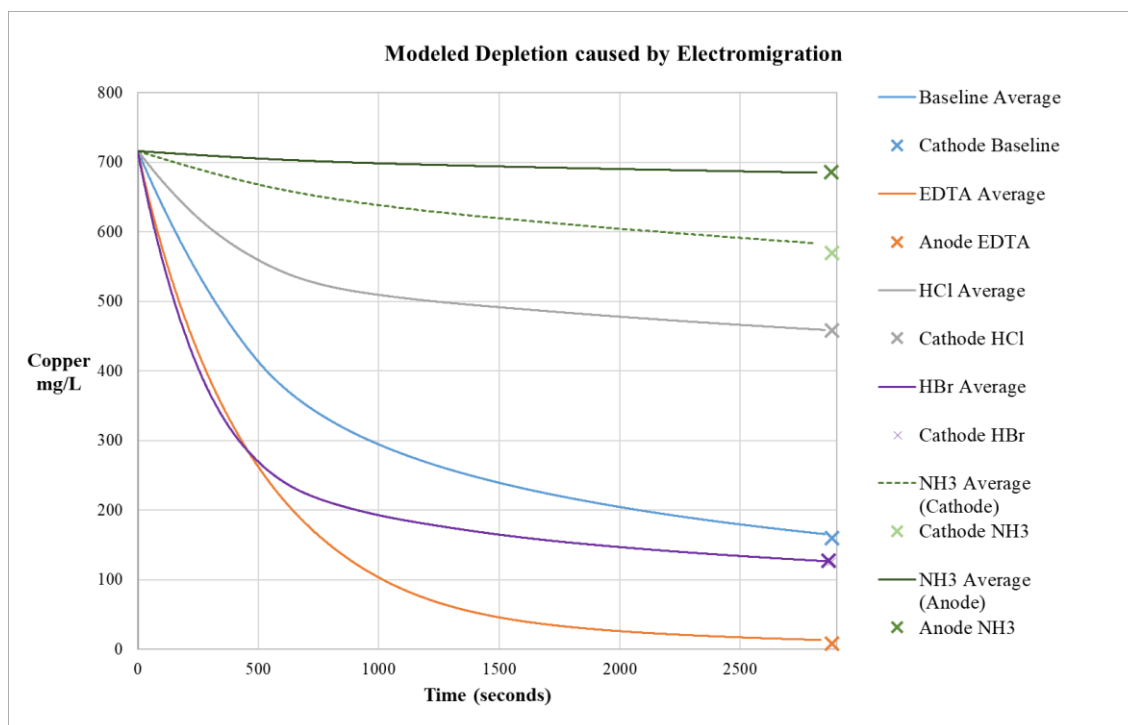


Figure 20. Modeled Depletion for each Complex Type.

The figure shows all the mass calculations for each type of experiment, using a dataset built from the average amperage values within each set of experiments. An apparent rate constant was selected by matching each depletion curve created by equation 9 to the known initial concentrations and final sampled ICP-MS concentrations inside the compartment, displayed as an “X”. The blue curve is a graph of the mass estimation in the cathode of the Baseline experiments, using a rate constant of -0.0008 . Similarly, the orange curve is a graph of the mass predictions for depletion in the anode compartment of the EDTA experiments, also using an apparent rate constant of -0.0008 . The grey curve shows the calculated mass depletion in the cathode compartment during the HCl experiments, using an apparent rate constant of -0.0006 . The purple curve is a graph of depletion in the cathode compartment during the HBr experiments, using an apparent rate constant of -0.00025 . Depletion was seen in both electrode compartments during the NH_3 experiments. Possible reasons for this result will be addressed in

the discussion section further on in this thesis. The light green is a graph of the depletion estimated in the cathode compartment during the NH_3 experiments, using a rate constant of -0.00006 . Lastly, the dark green curve is a graph of the depletion estimated in the anode compartment during the NH_3 experiments, using a rate constant of -0.000013 .

3.2.3. Electrode Compartment Enrichment

This section provides the results of the data analysis regarding the electrode compartment that was enriched. Unlike the depletion calculations of the previous section, these estimates use positive apparent rate constants to estimate the concentration in the electrode compartment opposite the ion charge. Figure 21 is graph of the enrichment estimated in the electrode compartments during the experiments. Similar to the figure on depletion, included on this figure are markers for the final compartment concentrations measured using ICP. This was the end point that the apparent rate constant was used to fit the model.

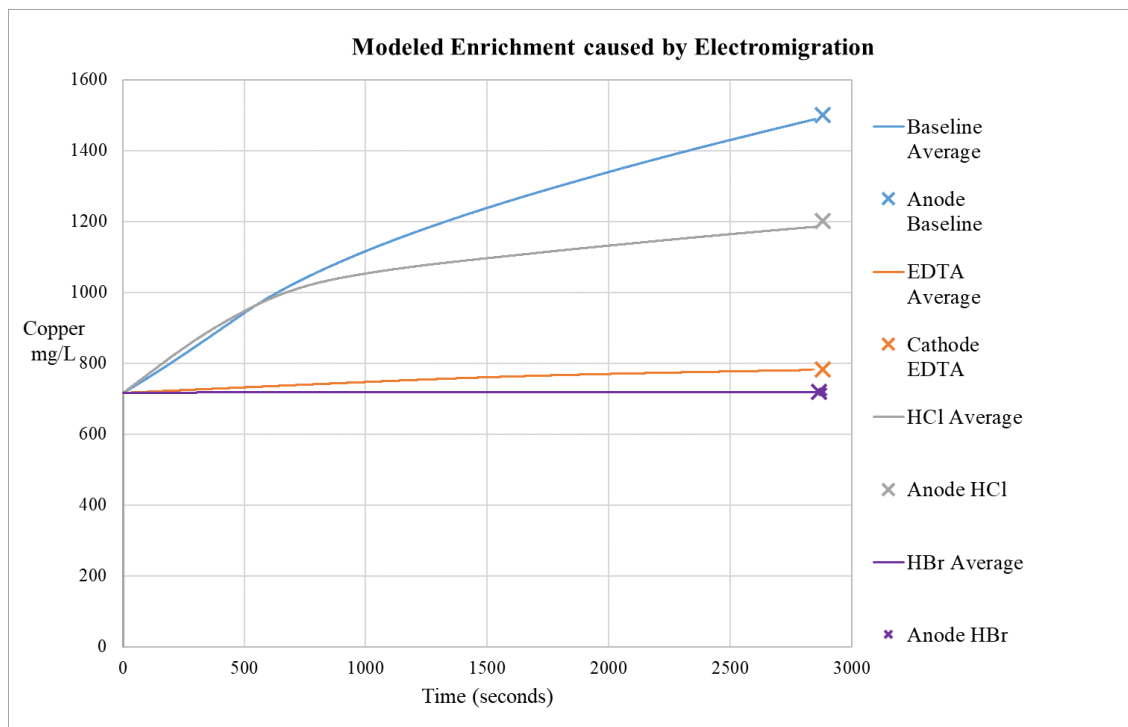


Figure 21. Modeled Enrichment for each Complex Type.

The blue curve shows the anode compartment during the Baseline copper sulfate experiments, using an apparent rate constant of 0.0004. The orange curve shows the estimated enrichment in the cathode compartment during the EDTA experiments, using an apparent rate constant of 0.00002. The gray curve is a graph of the estimated enrichment of copper in the anode compartment during the HCl experiments, using an apparent rate constant of 0.00007. Finally, purple curve is a graph of the estimated enrichment of copper in the anode compartment during the HBr experiments, using an apparent rate constant of 0.00000068.

Table II is a summary of the rate constants used for enrichment and depletion calculations for the five types of experiments conducted during this thesis, and the electrode compartments that enrichment and depletion were observed. It is important to note that the data analysis is empirical and has limitations in that it does not address mass losses to precipitation or electroplating. Also the effect of counter ions, such as sulfate, are not accounted for in this analysis. Counter ions such as sulfate effect the electrolyte flux within the reactor, and therefore cause changes in current. In the case of this data analysis, these current changes may be incorrectly attributed to changes resulting from copper transport.

Table II. Apparent rate constants used to calculate Enrichment and Depletion.

	Enrichment		Depletion	
	Apparent Rate Constant	Chamber	Apparent Rate Constant	Chamber
Baseline	0.0004	Anode	-0.0008	Cathode
EDTA	0.00002	Cathode	-0.0008	Anode
HCl	0.00007	Anode	-0.0006	Cathode
HBr	0.00000068	Anode	-0.00025	Anode
NH ₃ anode	-	-	-0.00006	Cathode
NH ₃ cathode	-	-	-0.000013	Anode

This table illustrates an interesting finding of this thesis, in that the expected direction of transport, based on initial charge, was not always observed in the experiments. For example, the copper bromide, and copper chloride complexes had initial charges of 2^- , indicating that transport and enrichment would be toward the cathode compartment, however following experiments, transport was seen to have been in the direction of the anode. This is further supported by the fact that there was no reduction of native copper on the steel cathode during the HCl and HBr experiments as was seen in the EDTA experiments, indicating that copper ions were not attracted to the cathode, as the initial charge would lead one to believe. Reasons for this will be further examined in the Discussion.

3.2.4. Observed Copper Transportation Rates

This section will provide the final results for copper transport rates that were calculated using the transport equation developed from the current data. A transport rate was calculated using equation 10 for the overall depletion and enrichment for each experiment type, as well as a transport rate for the initial 12.5 hours and final 35.5 hours of each experiment. Figure 22 below gives the concentration changes calculated for the baseline experiments.

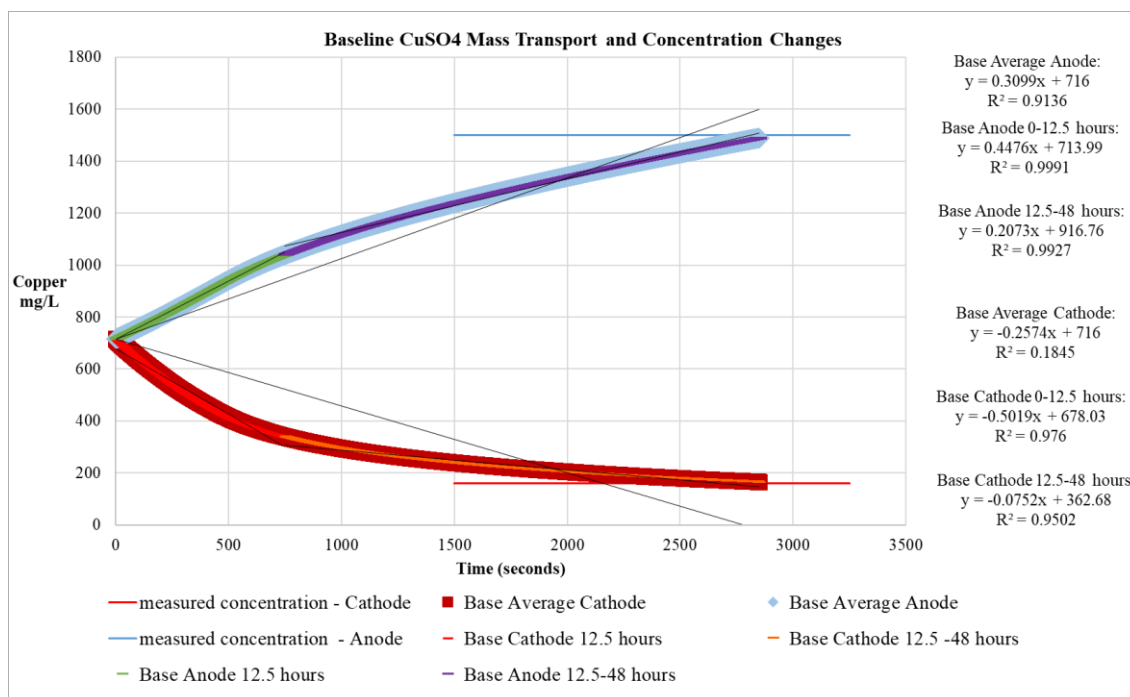


Figure 22. Baseline Concentration Changes.

The concentration changes were graphed from the average enrichment and depletion data sets from the baseline experiments. Figure 22 shows that the enrichment and depletion in the baseline experiments, was fairly symmetrical. As with all the EK runs, the initial 12.5 hours of the experiment were where the highest transport rates were seen. Following the first 12.5 hours, the transport velocity becomes more gradual.

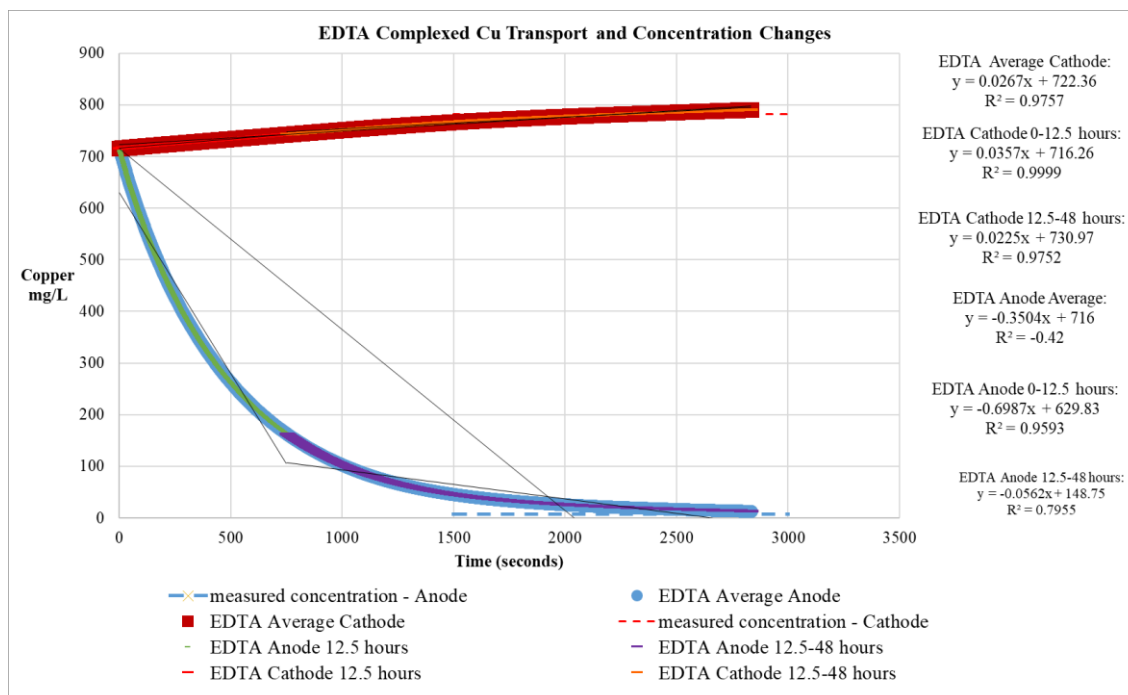


Figure 23. EDTA Complexed Copper Concentrations Changes.

Figure 23 shows the calculated concentration changes averaged in the EDTA experiments. This graph shows that the calculated depletion rates were much larger than the calculated enrichment rates. Again, this data displays the same rate change at 12.5 hours in both compartments, although the effect in depleting the anode compartment is more pronounced. As shown in the figure in section 3.1, there was significant reduction of native copper onto the cathode electrode during the EDTA experiments. The exact mass of reduced copper onto the electrodes was not qualified, and the ICP samples do not reflect this mass of copper, so the actual copper present in the cathode compartment is higher than Figure 23 depicts as “measured concentration-Cathode”.

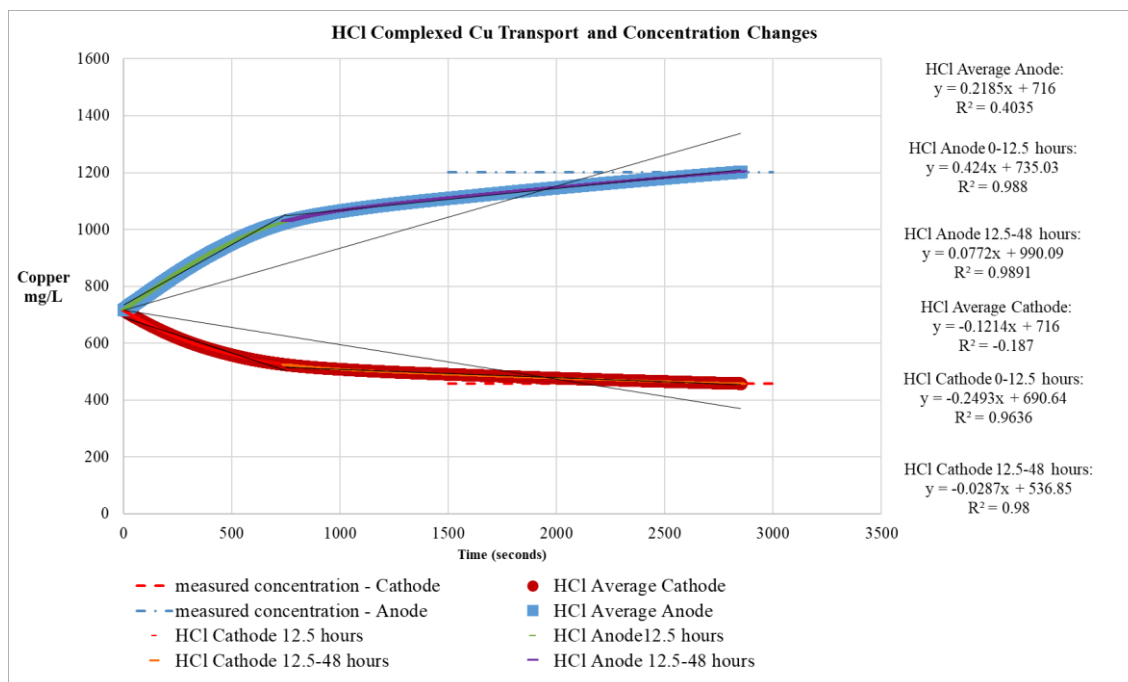


Figure 24. HCl Complexed Copper Concentrations Changes.

Figure 24 shows the calculated concentration changes averaged in the HCl experiments. Again, these experiments show symmetrical concentration changes in both electrode compartments, as well as a significant reduction of transport rates around the 12.5-hour mark. Unlike the previous figures, most of the copper transportation had been completed during the initial 12.5 hours of the experiment, with only a gradual change in concentration following.

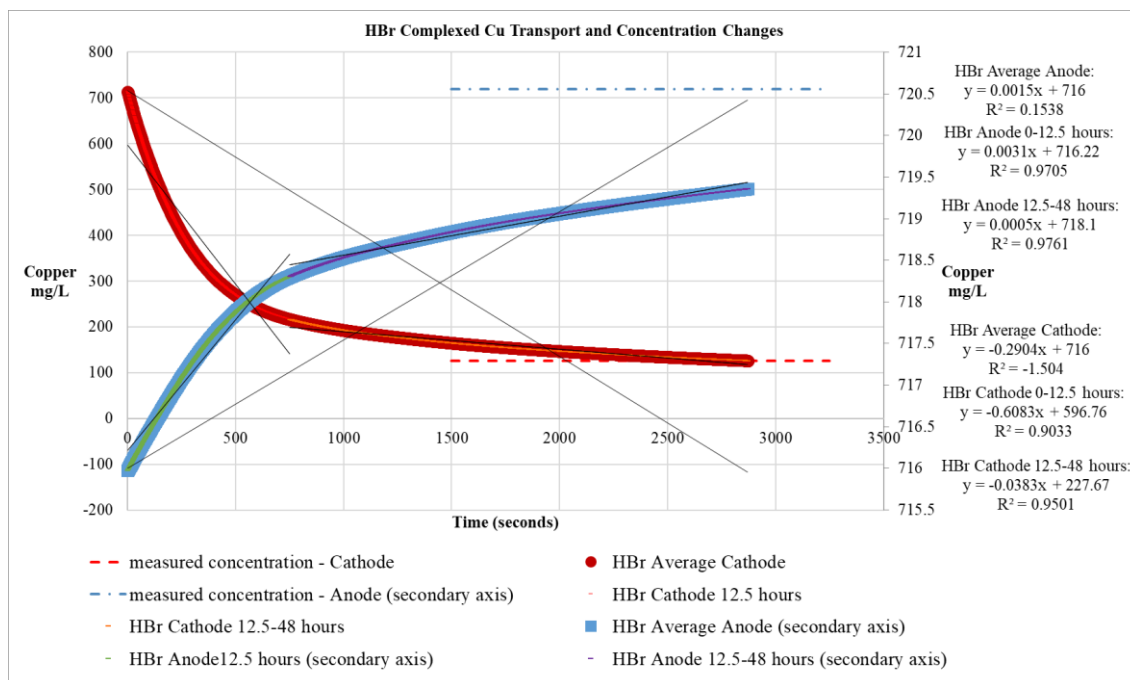


Figure 25. HBr Complexed Copper Concentrations Changes.

Figure 25 shows the concentration changes calculated during the HBr experiments, note the use of a secondary axis for the enrichment in the anode. Enrichment was not significantly seen during these experiments. Possible reasons for this will be addressed in the discussion. Again, the 12.5 hour rates reduction was seen, and similar to the HCl experiments, the majority of transport took place during the initial 12.5 hours.

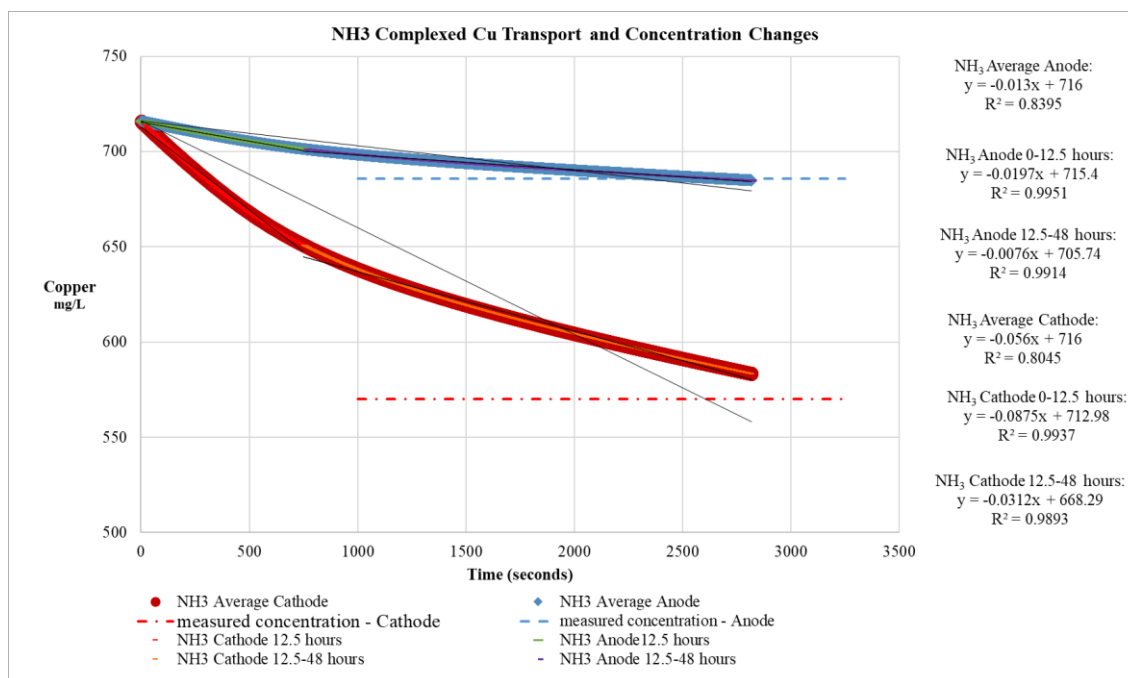


Figure 26. NH₃ Complexed Copper Concentrations Changes.

Lastly, Figure 36 shows the transport changes calculated in the anode and cathode compartments during the NH₃ experiments. Only depletion was observed during these experiments, and compared to the other experiments, these were low depletion rates. The poor performance of NH₃ may be due to the changing pH conditions caused by electrolysis creating conditions that did not favor a copper-ammonia complex. Figures 27 and 28 are graphs of the concentration changes calculated for the experiments, given in mg s^{-1} .

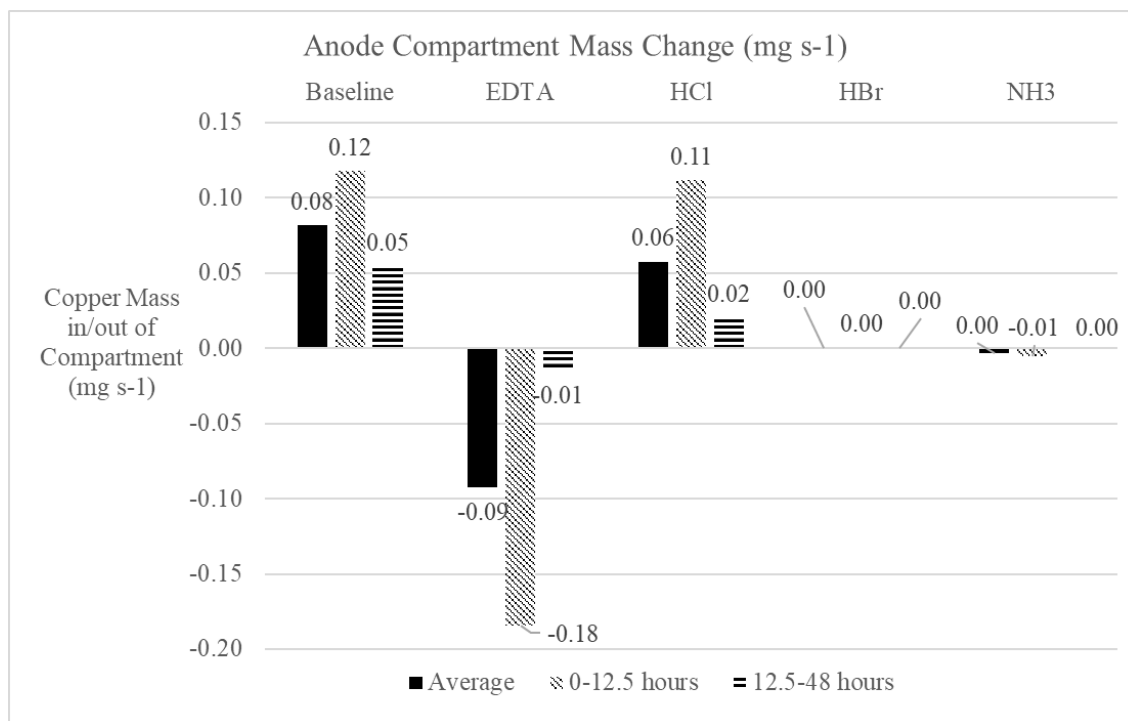


Figure 27. Anode Compartment Mass Change (mg s⁻¹).

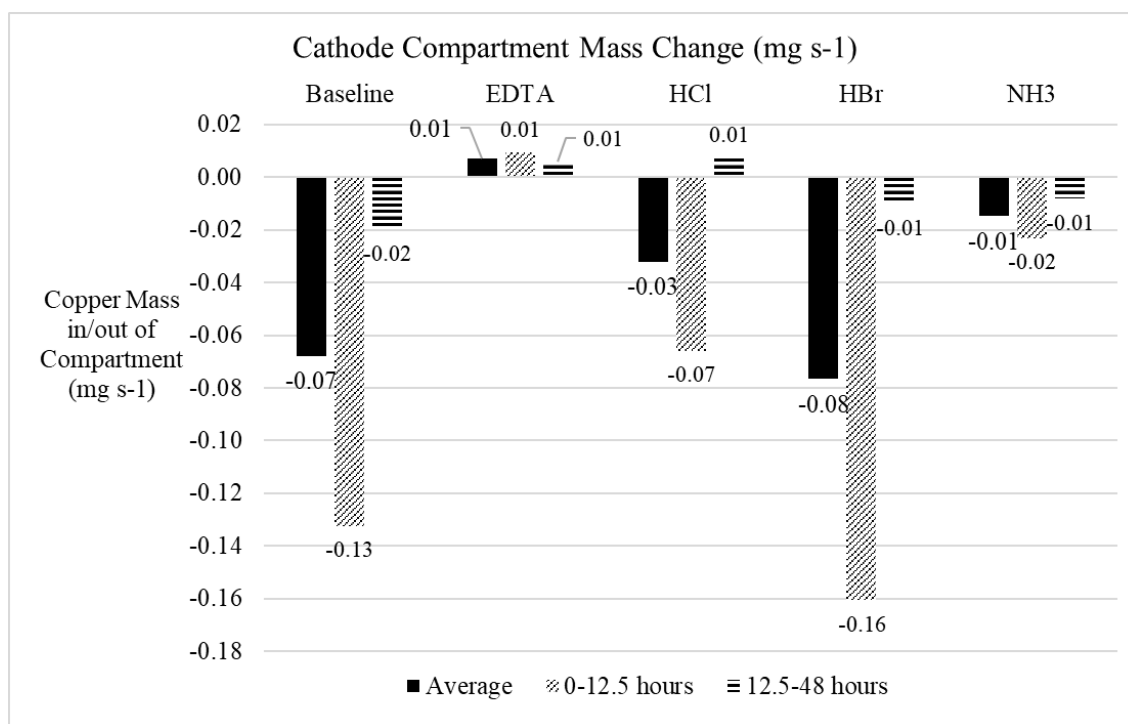


Figure 28. Cathode Compartment Mass Change (mg s⁻¹).

These values were calculated by multiplying the slope of the linear best fit lines ($\text{mg L}^{-1} \text{s}^{-1}$) and the electrode compartment volume (0.264 L) to calculate mass of copper entering the electrode compartment solution. The highest values for compartment enrichment were seen during the Baseline experiments, followed by the experiments using HCl as a complexing agent, then EDTA, and lastly using HBr. The largest values for depletion were calculated from the EDTA experiment, followed by the HBr, Baseline, and HCl experiments. Depletion rates in the NH_3 experiments were the slowest of all the trials, with depletion in the cathode being faster than in the anode.

4. Discussion

This section will discuss the results of this thesis project and areas of this experiment that could be improved and expanded upon. The initial portion of this discussion will focus on the experimental design of the thesis and how well it addressed the thesis goal of designing a project that produced replicable results at a laboratory scale. Following this discussion will be a section on the mass transport calculations and how well these calculations met the thesis goal of establishing the effect of complexing agent on transportation rates in an Electrokinetic Remediation system. Finally, a section will be devoted to what could be done by further work in the future. While much research remains to be done on how EK systems could be optimized to best remove contamination, EK remediation could be a viable technology for effectively removing heavy metal contamination in Butte, MT in areas where in-situ remediation is the only option.

4.1. Discussion on Experimental Design

The physical components of the experimental design of laboratory scale electrokinetic remediation reactors created for this thesis were a success in that they were simple to construct, affordable, durable, and allowed for consistent testing parameters to be maintained throughout the experiments. The scale of the reactors was also a success in that it allowed for a large number of experiments to be carried out without being overbearingly labor intensive. As mentioned in the methods section, the round PVC made consistent soil loading difficult, but with a little experience and by utilizing consistent loading techniques, it was possible to load each reactor with a consistent mass of soil each time. Also, the cheesecloth barriers were effective in keeping the soil and electrode compartments separate and maintaining constant volumes between experiments. The decontamination process developed in this thesis were also successful in

maintaining a clean laboratory and preventing cross contamination between experiments. The laboratory blank concentration was measured at 0.1 mg L^{-1} , which is not a relevant blank detection on the scale of the experiments were concentrations were far greater than ten times the blank detection.³⁷ The waste management was also an effective and easy way of disposing of waste without damaging the laboratory infrastructure or polluting the local wastewater treatment facility. The redox and mass accumulation onto electrodes however was unexpected and difficult to account for in the final mass transport calculations.

The software components of this project were also a success regarding project design. The National Instruments Data collection, power source and SPDT switch circuit were simple to assemble, and the program allowed for high resolution data collection over the course of the experiment that could be readily used in Excel or MATLAB.

4.2. The Effect of Complexing Agents on Transport Rates

This thesis produced mixed results on assessing the effect complexing agents have on the electromigration rates of copper in an Electrokinetic Remediation reactor. The complexing agents used were EDTA, HCl, HBr, and NH_3 and the basis behind this thesis goal was that complexing agents would increase the electromigration rates of copper because they replace water molecules that typically hydrate a copper ion. Complexing ions change the overall size of the ion and therefore change the drag component of the copper ion. Given this, the results should have shown that transport rates increase with a decrease in hydrated radius. In other words, the transport rates should have been highest in the bromide complex experiments, followed by

³⁷ US Environmental Protection Agency, *US EPA National Functional Guidelines for Inorganic Data Review* (2017), 56-59.

chloride, the hexaaqua copper complex, ammonia, and finally EDTA. However, this relationship was not seen. Instead, the highest rates of enrichment were seen in the baseline, hexaaqua copper complex experiments, followed by the chloride, EDTA, and bromide experiments. Furthermore, the highest depletion rates were observed in the EDTA experiments, followed by the bromide, hexaaqua copper, NH_3 and chloride experiments. Depletion and enrichment rates were determined using amperage data from all experiments, which consisted of three trials per complexing agent, and MS-ICP data from a subset of these trials. The fact that the rates of depletion and enrichment did not match one another within experiments is good evidence that the system parameters were changing inside the reactor, both spatially and temporally. The pH fronts in the reactor are likely causing the complexes to destabilize and convert into different hydrated ion complexes that have altered charge densities, geometries, and therefore have different transport velocities.

In addition to this, copper transport in the HCl and HBr experiments was not even in the direction that the ion complex charge would lead one to believe. In these experiments, the ions were initially complexed with four Cl^- or Br^- ions, resulting in an overall charge of 2^- however. Enrichment was seen in the anode compartment, meaning that the complex charge was changed to a positive value. This result lends to the conclusion that conditions in the reactor were changing in a way that this experiment did not anticipate. A likely cause for the reversal in charge is that the pH front caused by the electrolysis reactions at the electrodes created conditions in which the complex was no longer chemically stable. At this point it is possible that the Cl^- or Br^- ions were stripped off and replaced with water or OH^- molecules. Even before the ICP concentration tests were complete, there was evidence that charge reversal was happening, as native copper reduction was only observed on the EDTA experiment electrodes. EDTA forms

a very strong ligand bond with copper and it is possible that this strong bond was able to maintain stability through changing pH conditions. The HBr experiments also show greater signs of soil precipitation, see below in the left of Figure 29.

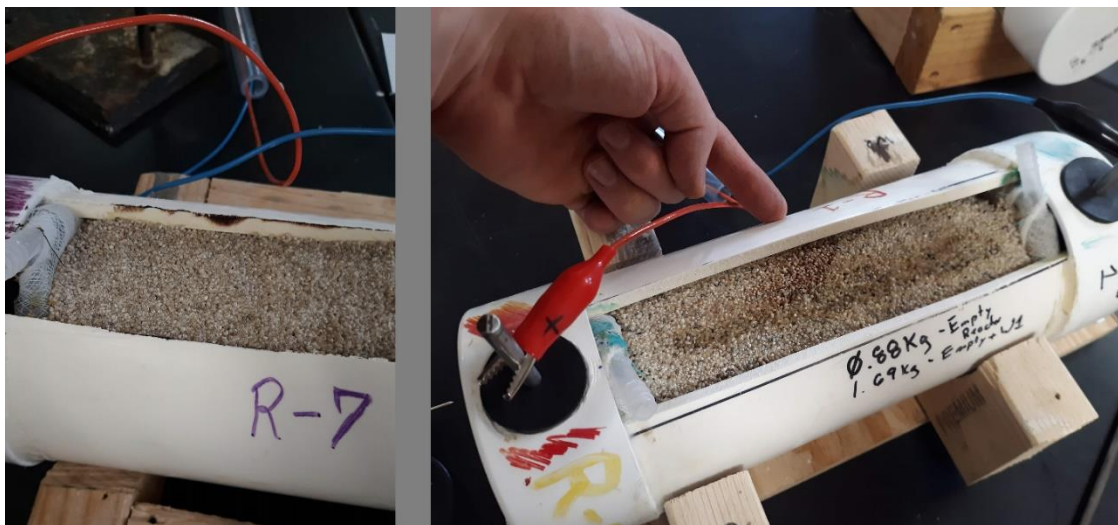
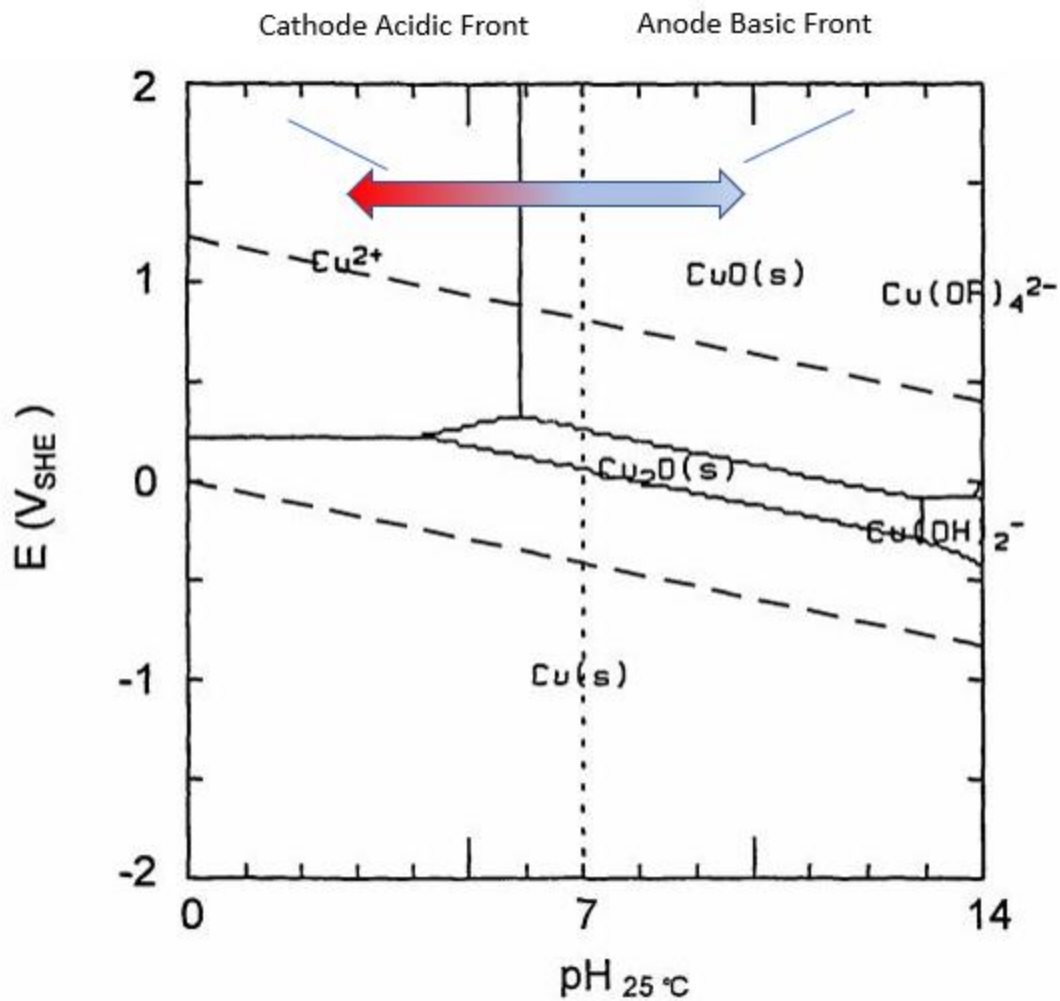


Figure 29. Right- NH₃ Reactor Precipitation. Left- HBr Reactor Precipitation.

The HBr reactors developed lateral discoloration streaks about 24-hours into the experiments. These were likely caused by precipitation brought on by changing pH concentrations. Similarly, the NH₃ experiments showed signs of precipitation caught in the sides of the reactors. Both point to evidence that the ligand bond strength of the complexing agent was not strong enough to stay stable through the changing pH conditions of the experiment.

Changing pH conditions were an unexpected challenge to this thesis and as the experiments progressed, it became evident that qualifying pH would be beneficial in determining the speciation, and solubility of the copper ions. The pH fronts were expected to cause precipitation; however, it is likely that the pH fronts also caused replacement reactions to occur on the complexes, altering their solubility, and transport properties. An attempt to quantify the pH changes was made by modifying the standard experimental setup with a pH probe that would collect readings per minute. However, this setup had two challenges that could not be overcome.

The pH probe itself is an electrode and functions on electrical currents, therefore it could not be housed directly in the electrode compartments and needed to be insulated separately from the system. This was accomplished by constructing a flow through cell that housed the probe in a beaker. Solution from the electrode compartment was pumped using a peristaltic pump in a way that would drip the solution into the cell so that the electric circuit was broken. The pump was run at a low rate to avoid disturbing the bulk solution. Unfortunately, the flow through cell was not successful in insulating the probe electrode for the entire course of the experiment, and pH readings were unreliable. It is likely that the dripping solution slowly crept up the cell walls and completed a circuit with the EK cell. This would either shut the probe off or cause obviously erroneous pH readings to be recorded. An attempt was made to increase the size of the flow through cell, but this resulted in larger mixing of the bulk fluid which washed out the effects of electromigration. Figure 30 below is a Pourbaix diagram of the speciation of copper ions in solution.



³⁸ Modified from Bjorn Beverskog, and Ignasi Puigdomenech, 1995.

Figure 30. Pourbaix Diagram of the Speciation of Copper Ions.

Transposed on top of this diagram is an arrow that shows the approximate changed to pH that occurred in the reactors during the EK experiments. Again, it is important to note that while the starting pH value was approximately 2.5, the final pH was unknown due to probe

³⁸ Bjorn Beverskog, and Ignasi Puigdomenech. *Revised Pourbaix diagrams for copper at 5-150 C.* (No. SKI-R--95-73. Swedish Nuclear Power Inspectorate, 1995), 2.

malfunctions. With this understanding, this graph does however show that the copper ions likely underwent speciation changes as they encountered the basic front near the anode.

Transport rates were highest during the initial 12.5 hours of the experiments. This effect was seen across all of the different trails. This is likely related to the current relationship given in equation 1 in the introduction. Transport was more efficient during the initial stage of the experiment because the solution was more homogenous. However, as the system progressed, the electrolyte deficient side of the reactor dampened the current that could travel through the reactor and the transport rates decreased. It is interesting that this effect was seen at a fairly regular time across the experiments.

4.3. Recommendations

While this thesis provided a strong start to experimental design of the physical reactors and a good start to the *in-situ* data collection during experiments, there are some areas that could be improved. As mentioned in the methods section of this work, a more rigorous soil loading technique could be implemented. This could take the form of a rectangular reactor of the same scale, or involve a PVP union joint that functioned as an electrode compartment. This would allow the researcher to more easily load the soil column.

The ICP sampling under sampled the electrode compartments. There was blue copper precipitation present on the cheesecloths following some of the reactor experiments. As stated in the methods, this solid matter was stirred up with the syringe during sampling, as an attempt to homogenize and capture it. However, it is likely that it was not fully accounted for and the actual concentration of copper in the compartments was higher than the ICP calculated. The recommendation for this drawback is to devise a sampling method that involves dissolving the precipitation to account for it in the sample. The difficulty lies in the fact that the cheesecloth

holds the soil column in place, and removing or tampering with it increases the risk of the soil caving. This would mix the electrode solution with solution in the soil column and alter the concentrations.

The data collected from this thesis was initial and final metal concentrations and real-time recording of current changes. This data was used to model changes in concentration and calculate transportation velocities. EK systems are incredibly dynamic and real time data collection is vital to being able to pinpoint changes within the reactors. A recommendation for future experimental setups is to expand on the possible real time data collected, such as measurements on pH and oxygen reduction potential so that the speciation of the metals can be better identified. An experiment would need to collect pH or oxygen reduction potential data at multiple points between the electrodes. The experiment would also need to devise a way to collect data in a way that did not cause the electric current to interfere with the probe sensors. This could be accomplished by submerging the probe in an insulated flow-through cell, although caution would need to be taken to ensure that the bulk fluid movement of the flow through cell did not disturb the electromigration rates.

4.4. Future Work

This work examined five different copper complexes, and the effect they had on transportation rates. However, over the course of the experiments, it became apparent that there were a number of areas in each experiment that could be further investigated. For example, each complexing agent had a particular relationship with the pH fronts that devolved during each experiment. A whole study could be devoted to understanding the stability of one complex, such as EDTA, over the course of an experiment. EDTA was one of the most intriguing complexes not

only because it demonstrated such high depletion rates, but also because it reduced native copper onto the cathode.

Likewise, a study could be devoted to determining the nature of the current drop seen so regularly at the 12.5 hour mark during the experiment. Possible factors to consider would be the initial concentration of metals in the reactor, or the voltage gradient used during the experiment. The study would be useful in determining the most efficient removal methods in terms of energy required and system run time.

4.5. Conclusion

Mine waste remediation is critical not only to the environmental quality, but to the health and standard of living of people living in areas impacted by historic or current mining activity. While excavation and large-scale treatment of mine waste will always be an effective solution, there is also a need for smaller scale, targeted *in-situ* remediation. Mine waste in communities such as Butte, MT is overlain with existing infrastructure that cannot be practically removed for excavation. Contamination like this is the motivation behind the work done for this thesis, and its research into improving *in-situ* remediation using electrokinetic systems. Electrokinetic remediation holds potential for improving the removal rates of heavy metal contamination. However, more work is needed to better understand the nuances and variables that influence an electrokinetic remediation system. This thesis developed a laboratory scale experiment that conducted research on how the transport rates of copper ions are affected by complexing ions. The experiments revealed that the transport rates are also affected by factors, such as pH changes, that were not fully qualified during the experiments. This thesis was, however, successful in that it developed some foundation work for future experiments and provided a simple design for EK reactors, waste management, and real time data collection.

5. Appendix A

Soil Mass Table

Test Type	Date	Mass of Reactor Empty (kg)	Mass of Reactor w/ Sand (kg)	Mass of sand (kg)	Mass of Reactor w/ Sand and Solution (kg)	Mass of Solution (kg)	Mass of Reactor post Experiment (kg)	Mass Loss Through Evaporation (kg)	
Baseline	1/24/2019	0.81	3.23	2.42	4.21	0.98	4.13	0.08	
Baseline	1/24/2019	0.77	3.17	2.4	4.2	1.03	4.15	0.05	
Baseline	1/29/2019	0.81	3.25	2.44	4.23	0.98	4.16	0.07	
Baseline	1/29/2019	0.77	3.17	2.4	4.16	0.99	4.08	0.08	
EDTA	2/19/2019	0.81	3.17	2.36	4.17	1.00	4.07	0.1	
EDTA	2/19/2019	0.77	3.06	2.29	4.07	1.01	3.98	0.09	
EDTA	2/26/2019	0.8	3.21	2.41	4.21	1.00	4.11	0.1	
HCl	2/26/2019	0.8	3.14	2.34	4.16	1.02	4.11	0.05	
HCl	3/3/2019	0.81	3.22	2.41	4.2	0.98	4.11	0.09	
HCl	3/3/2019	0.78	3.18	2.4	4.15	0.97	4.07	0.08	
HBr	3/5/2019	0.8	3.27	2.47	4.22	0.95	4.13	0.09	
HBr	3/5/2019	0.79	3.18	2.39	4.18	1.00	4.1	0.08	
HBr	3/10/2019	0.77	3.08	2.31	4.1	1.02	4.05	0.05	
NH ₃	3/15/2019	0.80	3.25	2.45	4.23	0.98	4.15	0.08	
NH ₃	3/15/2019	0.80	3.22	2.42	4.2	0.98	4.11	0.09	
Reactor Blank	3/15/2019	0.81	3.08	2.27	4.08	1.00	4.03	0.05	
NH ₃	3/20/2019	0.79	3.03	2.24	4.01	0.98	3.95	0.06	
						Maximum (kg)	2.47	1.03	0.1
						Minimum (kg)	2.24	0.95	0.05
						Standard Deviation	0.06	0.02	0.02
						Average (kg)	2.38	0.99	0.08

6. References Cited

- Superfund: National priorities list (NPL). in United States Government [database online]. 2017 [cited 01/10 2018]. Available from <https://www.epa.gov/superfund/superfund-national-priorities-list-npl>.
- Acar, Yalcin B., Robert J. Gale, Akram N. Alshawabkeh, Robert E. Marks, Susheel Puppala, Mark Bricka, and Randy Parker. 1995. Electrokinetic remediation: Basics and technology status. *Journal of Hazardous Materials* 40 (2): 117-37.
- Alexander, Charles K., and Matthew no Sadiku. 2000. Electric circuits. *Transformation* 135 : 4-5.
- Alshawabkeh, Akram N., and Yalcin B. Acar. 1996. Electrokinetic remediation. II: Theoretical model. *Journal of Geotechnical Engineering* 122 (3): 186-96.
- . 1996. Electrokinetic remediation. II: Theoretical model. *Journal of Geotechnical Engineering* 122 (3): 186-96.
- Ammami, MT, Florence Portet-Koltalo, Ahmed Benamar, C. Duclairoir-Poc, H. Wang, and F. Le Derf. 2015. Application of biosurfactants and periodic voltage gradient for enhanced electrokinetic remediation of metals and PAHs in dredged marine sediments. *Chemosphere* 125 : 1-8.
- Botz, Maxwell K. 1969. Hydrogeology of the upper silver bow creek drainage area, montana. Available from the Clearinghouse as Pb-193 025,\$ 0.65 in Microfiche.
- Beverkog, Björn, and Ignasi Puigdomenech. *Revised Pourbaix diagrams for copper at 5-150 C*. No. SKI-R--95-73. Swedish Nuclear Power Inspectorate, 1995.
- Chowdhury, Ahmed IA, Jason I. Gerhard, David Reynolds, Brent E. Sleep, and Denis M. O'Carroll. 2017. Electrokinetic-enhanced permanganate delivery and remediation of contaminated low permeability porous media. *Water Research* 113 : 215-22.
- Davis, Andy, and Daniel Ashenberg. 1989. The aqueous geochemistry of the berkeley pit, butte, montana, USA. *Applied Geochemistry* 4 (1): 23-36.
- Denisov, Gennady, R. Edwin Hicks, and Ronald F. Probst. 1996. On the kinetics of charged contaminant removal from soils using electric fields. *Journal of Colloid and Interface Science* 178 (1): 309-23.
- Gammons, Christopher H., and James P. Madison. 2006. Contaminated alluvial ground water in the butte summit valley. *Mine Water and the Environment* 25 (2): 124-9.

- Gammons, Christopher H., John J. Metesh, and Terence E. Duaine. 2006. An overview of the mining history and geology of butte, montana. *Mine Water and the Environment* 25 (2): 70-5.
- Gammons, Christopher H., Christopher L. Shope, and Terence E. Duaine. 2005. A 24 h investigation of the hydrogeochemistry of baseflow and stormwater in an urban area impacted by mining: Butte, montana. *Hydrological Processes: An International Journal* 19 (14): 2737-53.
- Impey, RW, PA Madden, and IR McDonald. 1983. Hydration and mobility of ions in solution. *The Journal of Physical Chemistry* 87 (25): 5071-83.
- Iyer, Ramasubramania. 2001. Electrokinetic remediation. *Particulate Science and Technology* 19 (3): 219-28.
- Kennelly, Patrick. 2011. Landscape volumetrics and visualizations of the butte mining district, montana. *Environmental & Engineering Geoscience* 17 (3): 213-26.
- Mao, Xuhui, James Wang, Ali Ciblak, Evan E. Cox, Charlotte Riis, Mads Terkelsen, David B. Gent, and Akram N. Alshawabkeh. 2012. Electrokinetic-enhanced bioaugmentation for remediation of chlorinated solvents contaminated clay. *Journal of Hazardous Materials* 213 : 311-7.
- Mulligan, CN, RN Yong, and BF Gibbs. 2001. Remediation technologies for metal-contaminated soils and groundwater: An evaluation. *Engineering Geology* 60 (1-4): 193-207.
- Newman, John, and Karen E. Thomas-Alyea. 2012. *Electrochemical systems* John Wiley & Sons.
- Puppala, Susheel K., Akram N. Alshawabkeh, Yalcin B. Acar, Robert J. Gale, and Mark Bricka. 1997. Enhanced electrokinetic remediation of high sorption capacity soil. *Journal of Hazardous Materials* 55 (1-3): 203-20.
- Ribeiro, AB, JM Rodriguez-Maroto, EP Mateus, and H. Gomes. 2005. Removal of organic contaminants from soils by an electrokinetic process: The case of atrazine.: Experimental and modeling. *Chemosphere* 59 (9): 1229-39.
- Rosestolato, Davide, Roberto Bagatin, and Sergio Ferro. 2015. Electrokinetic remediation of soils polluted by heavy metals (mercury in particular). *Chemical Engineering Journal* 264 : 16-23.
- Sandu, Ciprian, Marius Popescu, Emilio Rosales, Marta Pazos, Gabriel Lazar, and M. Ángeles Sanromán. 2017. Electrokinetic oxidant soil flushing: A solution for in situ remediation of hydrocarbons polluted soils. *Journal of Electroanalytical Chemistry* 799 : 1-8.

- See, Ronald F., Rebecca A. Kruse, and William M. Strub. 1998. Metal– ligand bond distances in first-row transition metal coordination compounds: Coordination number, oxidation state, and specific ligand effects. *Inorganic Chemistry* 37 (20): 5369-75.
- Souza, FL, C. Saéz, J. Llanos, MRV Lanza, P. Cañizares, and MA Rodrigo. 2016. Solar-powered electrokinetic remediation for the treatment of soil polluted with the herbicide 2, 4-D. *Electrochimica Acta* 190 : 371-7.
- . 2016. Solar-powered electrokinetic remediation for the treatment of soil polluted with the herbicide 2, 4-D. *Electrochimica Acta* 190 : 371-7.
- US Environmental Protection Agency. 1994. US EPA contract laboratory program national functional guidelines for inorganic data review.
- Villen-Guzman, Maria, Juan M. Paz-Garcia, Jose M. Rodriguez-Maroto, Francisco Garcia-Herruzo, Gema Amaya-Santos, Cesar Gomez-Lahoz, and Carlos Vereda-Alonso. 2015. Scaling-up the acid-enhanced electrokinetic remediation of a real contaminated soil. *Electrochimica Acta* 181 : 139-45.
- Virkutyte, Jurate, Mika Sillanpää, and Petri Latostenmaa. 2002. Electrokinetic soil remediation—critical overview. *Science of the Total Environment* 289 (1): 97-121.
- Yang, Gordon C. C., and Yu-Wen Long. 1999. *Removal and degradation of phenol in a saturated flow by in-situ electrokinetic remediation and fenton-like process*. Vol. 69.
- Yao, Zhitong, Jinhui Li, Henghua Xie, and Conghai Yu. 2012. Review on remediation technologies of soil contaminated by heavy metals. *Procedia Environmental Sciences* 16 : 722-9.
- . 2012. Review on remediation technologies of soil contaminated by heavy metals. *Procedia Environmental Sciences* 16 : 722-9.
- Yeung, Albert T. 2011. Milestone developments, myths, and future directions of electrokinetic remediation. *Separation and Purification Technology* 79 (2): 124-32.
- Yuan, Lizhu, Xingjian Xu, Haiyan Li, Quanying Wang, Nana Wang, and Hongwen Yu. 2017. The influence of macroelements on energy consumption during periodic power electrokinetic remediation of heavy metals contaminated black soil. *Electrochimica Acta* 235 : 604-12.
- Zhao, Shuning, Li Fan, Mingyuan Zhou, Xuefeng Zhu, and Xiuli Li. 2016. Remediation of copper contaminated kaolin by electrokinetics coupled with permeable reactive barrier. *Procedia Environmental Sciences* 31 : 274-9.

SIGNATURE PAGE

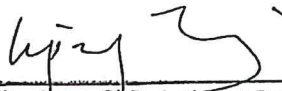
This is to certify that the thesis prepared by Timothy Driscoll entitled "Enhancing the Efficiency of Electrokinetic Remediation through the use of Complexing Agents" has been examined and approved for acceptance by the Department of Environmental Engineering, Montana Technological University, on this 8th day of July, 2019.



Xufei Yang, PhD, Assistant Professor
Department of Environmental Engineering
Chair, Examination Committee



Katherine R. Zodrow, PhD, Associate Professor and Department Head
Department of Environmental Engineering
Member, Examination Committee



Liping Jang, PhD, Assistant Professor
Department of Civil Engineering
Member, Examination Committee



Kim Snodgrass, PE, MS
Water and Environmental Technologies
Member, Examination Committee